Stem Cell Reports
Article

OPEN ACCESS

Endogenous WNT Signaling Regulates hPSC-Derived Neural Progenitor Cell Heterogeneity and Specifies Their Regional Identity

Noel Moya,[1,4] Josh Cutts,[1,2,4] Terry Gaasterland,[3] Karl Willert,[1,*] and David A. Brafman[1,2,*]
[1]Department of Cellular and Molecular Medicine, Stem Cell Program, University of California, San Diego, 9500 Gilman Drive, La Jolla, CA 92093-0695, USA
[2]School of Biological and Health Systems Engineering, Arizona State University, Tempe, AZ 85287-9709, USA
[3]UCSD and Scripps Institution of Oceanography, Scripps Genome Center, 9500 Gilman Drive, La Jolla, CA 92093-0202, USA
[4]Co-first author
*Correspondence: kwillert@ucsd.edu (K.W.), david.brafman@asu.edu (D.A.B.)
http://dx.doi.org/10.1016/j.stemcr.2014.10.004

SUMMARY

Neural progenitor cells (NPCs) derived from human pluripotent stem cells (hPSCs) are a multipotent cell population that is capable of nearly indefinite expansion and subsequent differentiation into the various neuronal and supporting cell types that comprise the CNS. However, current protocols for differentiating NPCs toward neuronal lineages result in a mixture of neurons from various regions of the CNS. In this study, we determined that endogenous WNT signaling is a primary contributor to the heterogeneity observed in NPC cultures and neuronal differentiation. Furthermore, exogenous manipulation of WNT signaling during neural differentiation, through either activation or inhibition, reduces this heterogeneity in NPC cultures, thereby promoting the formation of regionally homogeneous NPC and neuronal cultures. The ability to manipulate WNT signaling to generate regionally specific NPCs and neurons will be useful for studying human neural development and will greatly enhance the translational potential of hPSCs for neural-related therapies.

INTRODUCTION

Neural progenitor cells (NPCs) and neurons derived from human pluripotent stem cells (hPSCs) could provide an unlimited source of cells for drug testing and cell-based therapies (Koch et al., 2009; Zhang et al., 2008). In addition, these cells provide a unique opportunity to explore complex neural development in a simplified and accessible system. Current protocols for differentiating hPSCs toward specific neuronal lineages result in a mixture of neurons from various regions of the CNS, which limits the use of these cells for cell-based therapies, disease modeling, and developmental studies that require uniform populations of neurons. However, the precise source of this heterogeneity in neuronal cultures has yet to be resolved.

Differentiation of stem and progenitor populations is largely governed by the heterogeneity present in these cultures, which ultimately determines their differentiation bias. For example, several studies have found subpopulations with distinct self-renewal and differentiation potentials in hematopoietic (Dykstra et al., 2007; Huang et al., 2007) and intestinal (Sangiorgi and Capecchi, 2008) stem cells. Likewise, heterogeneous expression of pluripotency-related transcription factors and other cell-surface markers bestows distinct lineage-specific differentiation propensities on hPSCs (Drukker et al., 2012; Hong et al., 2011; Narsinh et al., 2011; Stewart et al., 2006; Wu and Tzanakakis, 2012). In contrast, NPCs derived from hPSCs have been considered to be a homogeneous cell population, and it has been suggested that their differentiation to neuronal cultures can be biased and manipulated by altering culture conditions (Dottori and Pera, 2008; Gaspard and Vanderhaeghen, 2010; Germain et al., 2010; Jiang et al., 2012; Liu and Zhang, 2011; Nat and Dechant, 2011; Peljto and Wichterle, 2011; Zhang, 2006). Our study challenges this simplistic view of neuronal differentiation in hPSC cultures.

We demonstrate that hPSC-derived NPCs, like other stem and progenitor populations, are heterogeneous and display a bias in their differentiation potential. Through the use of WNT reporter hPSC lines, we identified endogenous WNT signaling as a primary regulator of this heterogeneity in NPC and neuronal cultures. Flow cytometry (FC)-based purification and genetic assessment of reporter-expressing cell types revealed that the identity and differentiation potential of hPSC-derived NPCs are directly related to the level of endogenous WNT signaling present in these cell types. Through exogenous manipulation of WNT signaling, we were able to reduce NPC heterogeneity and generate cultures of regionally specific progenitors and neurons. Overall, this study demonstrates that WNT signaling plays an important role in deriving regionally homogeneous populations of NPCs and neurons, thereby greatly improving their scientific and therapeutic utility.

RESULTS

Endogenous WNT Signaling Is a Major Source of Heterogeneity in NPCs Derived from hPSCs

It is well established that WNT signaling regulates the regional identity along the anterior-posterior (A/P) axis of

the developing CNS. To explore the possibility that WNT signaling exerts similar effects in a cell-culture-based system of neural development, we generated clonal human embryonic stem cell (hESC) lines (HUES9) carrying a stably integrated GFP reporter under the control of a WNT-responsive promoter, called TCF Optimal Promoter (TOP (Fuerer and Nusse, 2010) (Figure S1A available online). In undifferentiated hESCs, this reporter is inactive but expresses GFP upon stimulation with recombinant WNT3a (Figure S1B). In contrast to a previous study (Blauwkamp et al., 2012), none of our clones or the nonclonal pool expressed GFP in the absence of exogenous WNT3a. This likely reflects the heterogeneity among hESC lines, especially with respect to endogenous expression of WNT3 (Jiang et al., 2013). In a subsequent analysis we focused on one clone, clone 19 (hTOP-19), which exhibited robust GFP expression upon WNT3a stimulation (nearly 100%; Figure S1B), displayed a normal female karyotype of 46 chromosomes (Figure S1C), and responded to various concentrations of exogenously added WNT3a (Figure S1D) and chemical inhibitors of GSK3β, such as BIO (Figure S1E).

Upon differentiation of this WNT reporter line to NPCs (Brafman, 2014) (Figure S2A), we observed a heterogeneous pattern of GFP expression in the absence of any exogenously added WNT proteins (Figure 1A). Despite uniform expression of the pan-neural markers SOX1, SOX2, and NESTIN (Figures S2B and S2C), and cell morphology (Figure S2D), FC revealed that GFP expression peaked upon rosette formation and a stable population of GFP-positive (GFP^+) cells persisted through subsequent NPC passages (Figure 1B). Addition of WNT3a to these NPC cultures resulted in uniformly high GFP expression, thereby demonstrating a homogeneous response to WNT signaling in this clonally derived population (Figure S1F). Furthermore, inhibiting endogenous WNT signaling with IWP2, a small molecule that acts on PORCN to block WNT processing and subsequent secretion (Chen et al., 2009), eliminated GFP expression, confirming that reporter expression was due to endogenous WNT signaling (Figure S1F).

Consistent with this heterogeneous expression of WNT reporter activity and with previously published studies (Dottori and Pera, 2008; Gaspard and Vanderhaeghen, 2010; Germain et al., 2010; Jiang et al., 2012; Liu and Zhang, 2011; Nat and Dechant, 2011; Peljto and Wichterle, 2011; Zhang, 2006), we found that NPCs derived under this protocol exhibited significant heterogeneity with respect to regionally specific markers (Figures S2E–S2H) despite uniform expression of the pan-neural markers SOX1 and SOX2 (Figures S2B and S2C). For example, these NPCs expressed markers of all A/P regions, including the forebrain (*FOXG1* and *DLX2*), forebrain/midbrain (*OTX2*), midbrain/hindbrain (*EN1* and *IRX3*), and hindbrain/spinal cord (*HOXB4*) (Figure S2E). Moreover, single-cell analysis by FC and immunofluorescence (IF) revealed that our NPC cultures heterogeneously expressed the regionally specific markers FORSE-1 (Figure S2F; forebrain), PAX6 (Figure S2G), and HOXB4 (Figure S2H). Together, these data suggested that these in vitro NPC cultures, as in the developing embryo (Pevny et al., 1998; Uwanogho et al., 1995; Wood and Episkopou, 1999), are exposed to patterning cues that impart distinct regional identities and neuronal differentiation potentials. Additionally, we confirmed that these NPCs were able to differentiate to neurons (Figures S2I–S2K), including those with a GABAergic identity (Figure S2J), and glial cells (Figure S2K).

To investigate the extent to which the high degree of heterogeneity in A/P positional identity correlated with our observed heterogeneity in WNT reporter activity, we performed whole transcriptome RNA sequencing (RNA-seq) on sorted GFP^+ and GFP-negative (GFP^-) NPCs from passage 5 NPC cultures (Table S1). Overall, we identified 1,273 genes with statistically significant differential expression between these two cell populations, with expression of 707 genes being elevated in the GFP^+ population and 566 genes elevated in the GFP^- population (Figure 1C; Table S1). As expected, WNT target genes such as *SP5*, *LEF1*, and *AXIN2* were elevated in the GFP^+ population (Figure 1D; Table S2). Additional analysis of WNT pathway components revealed that expression of the majority of WNT proteins and agonists was higher in GFP^+ NPCs, whereas expression of WNT antagonists was higher in GFP^- NPCs (Figure 1D; Table S2).

Furthermore, expression of genes with distinct domains of expression along the A/P axis segregated into these two cell populations (Figure 1E; Table S3). Specifically, we found that GFP^- NPCs in clone hTOP-19 were enriched for forebrain/anterior-specific markers such as *LHX8*, *DLX2*, *FOXG1*, and *LHX2*. Conversely, the expression of hindbrain/posterior-related markers such as *GBX2*, *PITX2*, *FGF8*, and *IRX3* was increased in GFP^+ NPCs. Most notably, members of the *HOX* gene family, which are highly expressed in the hindbrain and spinal cord, were significantly upregulated in the GFP^+ cell population. Finally, various midbrain-associated genes such as *EN1*, *EN2*, *LMX1A*, and *LMX1B* were expressed in both populations. Collectively, this RNA-seq analysis establishes a correlation between cells that receive a WNT signal (i.e., the GFP^+ population) and posterior fates. In contrast, NPCs that do not receive an endogenous WNT signal input (i.e., the GFP^- population) are biased toward an anterior identity.

To further characterize the diversity of cells expressing varying levels of GFP in the hTOP-19 NPCs, we used FC to isolate GFP^{HIGH}, GFP^{MID}, and GFP^{LOW} populations (Figure 2A). After cell sorting, the specific level of GFP expression remained stable in subsequent culture (Figure 2B). As expected, expression of the WNT target gene *AXIN2* was

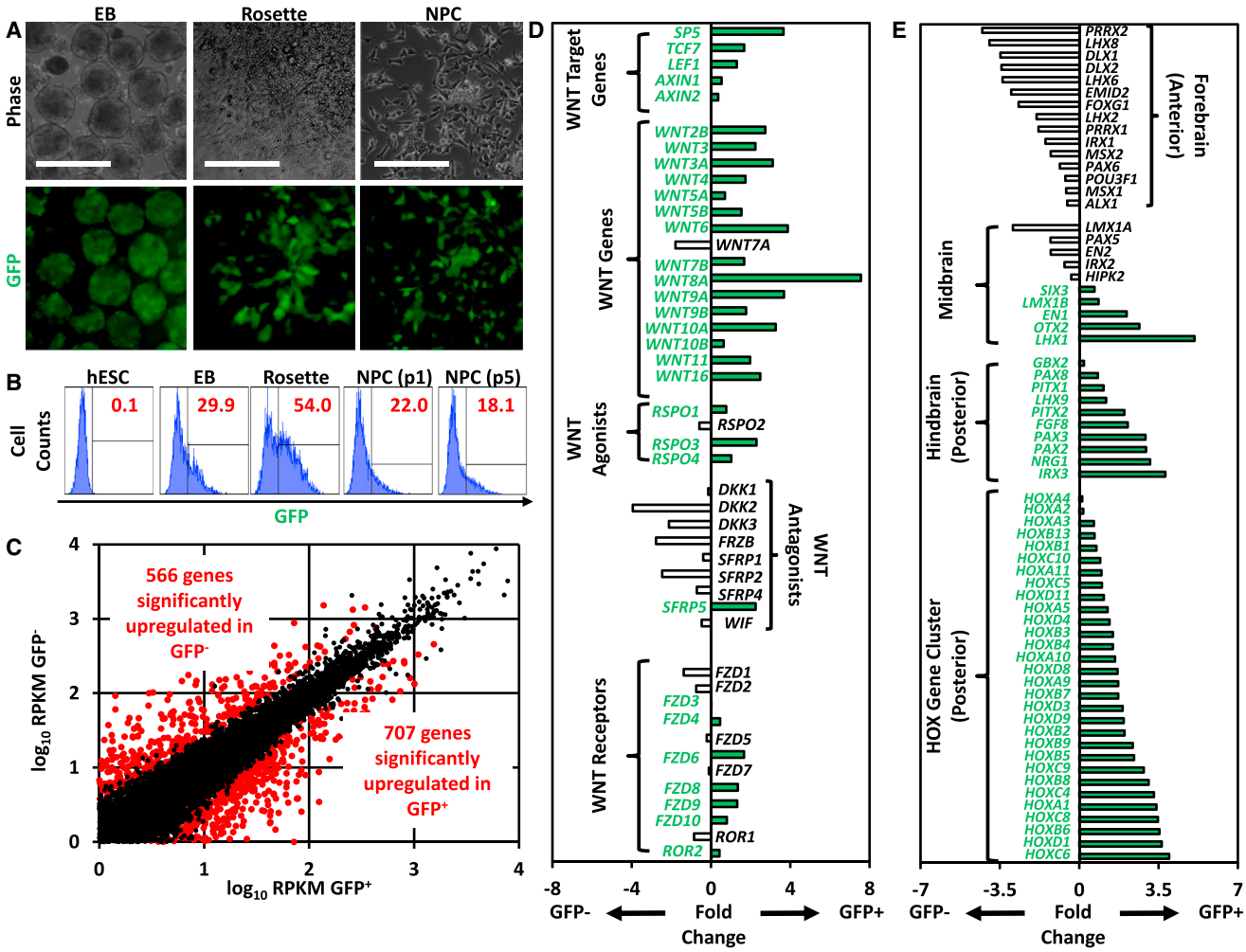

Figure 1. NPCs Are Heterogeneous with Respect to Endogenous WNT Signaling

(A) Phase contrast and fluorescent images of WNT reporter hESCs during neural differentiation (EB, scale bar, 500 μm; rosette and NPC, scale bar, 200 μm).

(B) FC of WNT reporter hESCs during neural differentiation. No detectable GFP signal was observed in hESCs, but upon differentiation to NPCs, a range of GFP expression patterns was observed. A population of GFP^+ cells endured through multiple NPC passages.

(C) Passage 5 reporter-expressing NPCs were separated by FC on the basis of GFP expression. A scatterplot of $\log_{10}$ RPKM in GFP^+ and GFP^- NPCs is shown. Genes with statistically significant differences in expression are shown in red.

(D and E) Selection of differentially expressed genes highlighting differences in gene-expression patterns related to (D) WNT signaling and (E) A/P patterning and differentiation of the neural tube.

See also Figures S1 and S2 and Tables S1, S2, and S3.

highest in the GFP^{HIGH} cell population and lowest in the GFP^{LOW} NPCs (Figure 2C). The three sorted cell populations expressed similar levels of the pan-neural markers SOX1, SOX2, and NESTIN (Figures 2D, S3A, and S3B), demonstrating that NPCs of varying endogenous WNT activity are homogeneous with respect to expression of pan-neural markers.

We examined the A/P expression profile (Figure 2E) of NPCs with different levels of endogenous WNT signaling by quantitative PCR (qPCR; Figure 2F), IF (Figure 2G), and FC (Figures 2H and 2I). Expression of the forebrain markers *FOXG1*, *SIX3*, and *DLX2* was highest in GFP^{LOW} NPCs. Expression of *OTX2*, which is expressed at the forebrain-midbrain boundary, was similar in the GFP^{LOW} and GFP^{MID} populations but absent in the GFP^{HIGH} NPCs. Expression of the midbrain marker *LMX1A* was highest in the GFP^{MID} population. The midbrain/hindbrain boundary markers *IRX3* and *EN1* were expressed at high levels in both the GFP^{MID}- and GFP^{HIGH}-sorted cell populations. The hindbrain markers HOXA2 and HOXB4 were highly expressed

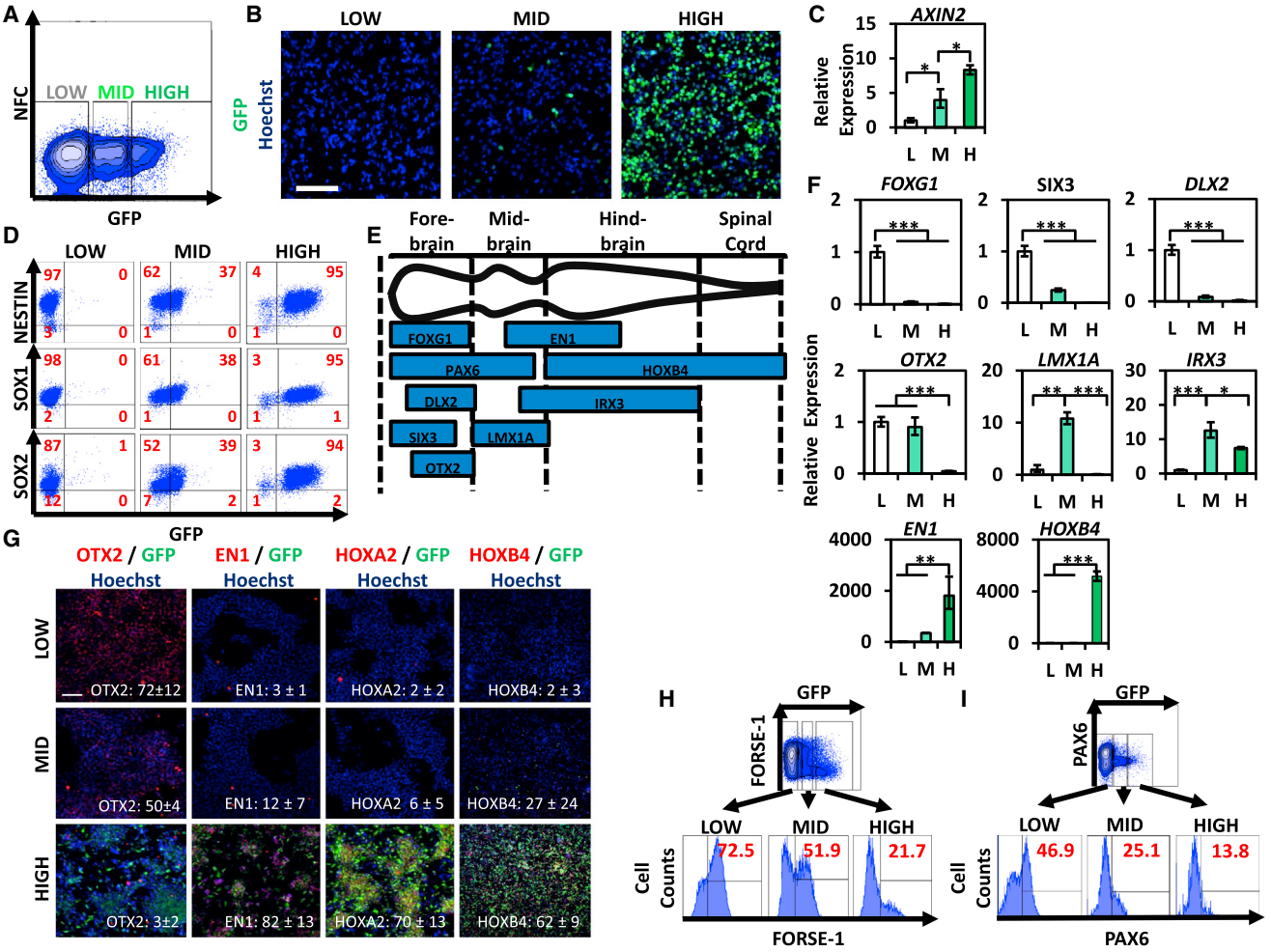

Figure 2. Characterization of WNT Reporter-Expressing NPC Populations Reveals a Regional Bias

(A) WNT reporter NPCs were divided into three populations on the basis of GFP expression: GFP^{LOW}, GFP^{MID}, and GFP^{HIGH}.

(B) Fluorescent images of GFP-sorted NPC populations. GFP expression remains stable after sorting and subsequent culture (scale bar, 100 μm).

(C) Gene expression of the WNT target gene *AXIN2* in GFP-sorted NPC populations (mean ± SEM, n = 3 independent experiments).

(D) FC of the pan-neural markers NESTIN, SOX1, and SOX2 in GFP-sorted NPC populations.

(E) Schematic of areas of expression of key genes involved in A/P patterning of the developing neural tube.

(F) Gene-expression analysis of A/P-related genes in GFP-sorted NPC populations (mean ± SEM, n = 3 independent experiments). Populations were compared using Student's t test. *p < 0.05, **p < 0.01, ***p < 0.001.

(G) IF of A/P-related markers in GFP expression in GFP^{LOW}, GFP^{MID}, and GFP^{HIGH} (scale bar, 100 μm).

(H and I) FC of (H) FORSE-1 and (I) PAX6 expression in unsorted and sorted GFP-expressing NPC populations. Isotype controls used are listed in Table S5. NFC, nonfluorescing channel.

See also Figure S3.

in the GFP^{HIGH} NPCs and diminished in both the GFP^{MID} and GFP^{LOW} populations. Finally, we performed FC on unsorted GFP-expressing hTOP-19 NPCs. This analysis demonstrated a negative correlation between GFP levels and expression of the anterior neural cell-surface marker FORSE-1 (Elkabetz et al., 2008) (Figure 2H). PAX6, which is expressed in the diencephalon and midbrain during early development, was expressed primarily in the GFP^{LOW} and GFP^{MID} cell fractions (Figure 2I). Together, these data suggest that the level of endogenous WNT signaling correlates with the positional identity of hESC-derived NPCs.

To determine whether the effect of endogenous WNT signaling on the regional patterning of NPCs was stable, we cultured sorted GFP^{HIGH} and GFP^{LOW} populations for ten passages (>50 days) and examined the expression of A/P-related genes (Figure S3C). Expression of *AXIN2*

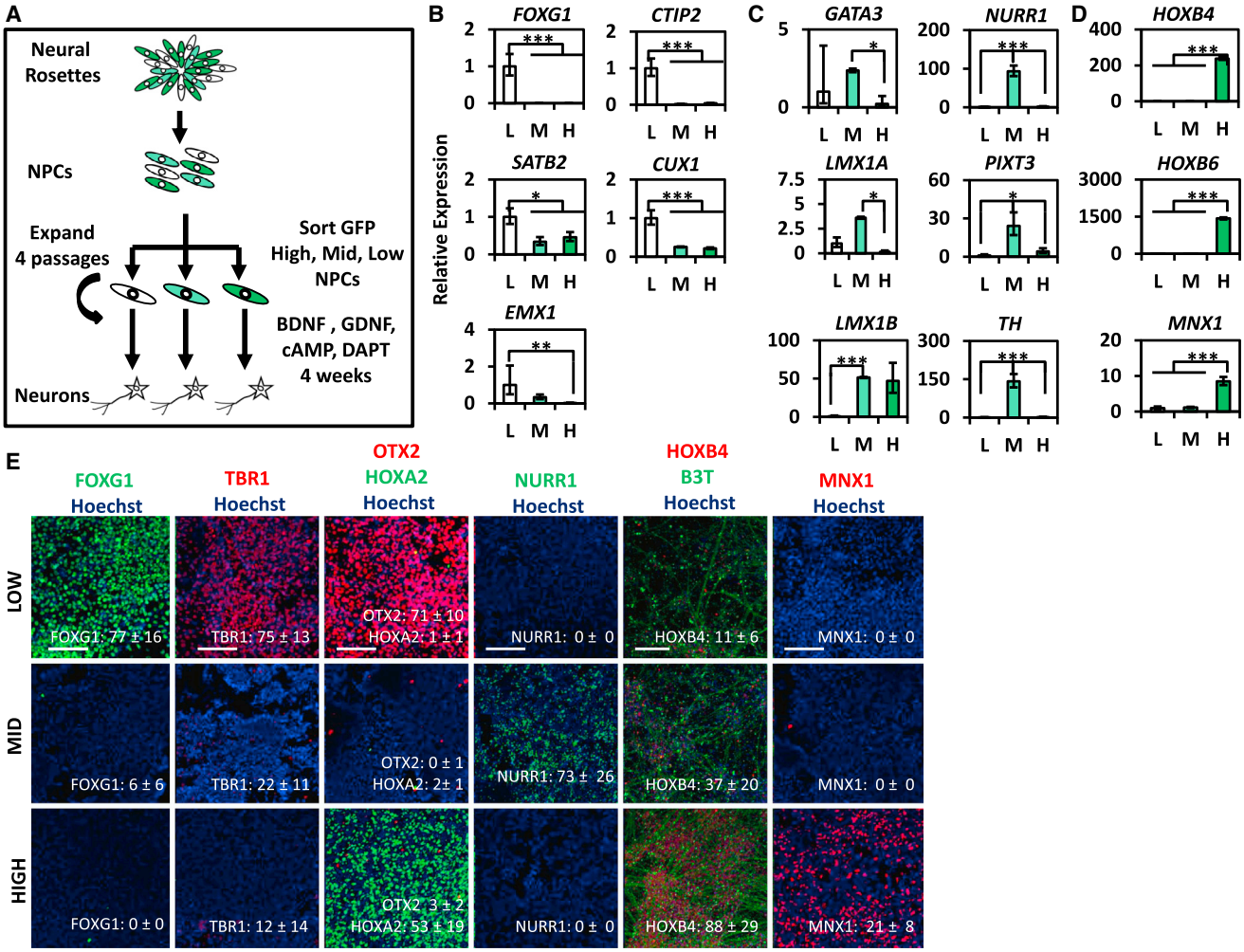

Figure 3. Neuronal Differentiation Bias of Sorted GFP-Expressing NPC Populations

(A) Schematic of the experimental protocol. FC was used to sort GFP-expressing NPCs into GFP^{LOW}, GFP^{MID}, and GFP^{HIGH} populations. The sorted cell populations were expanded for four passages and then differentiated to neurons.

(B–D) Gene-expression analysis of (B) cortical/forebrain-, (C) midbrain-, and (D) hindbrain/spinal-cord-related neuronal genes in neurons derived from sorted GFP-expressing NPC populations (mean ± SEM, n = 4 independent experiments). Populations were compared using Student's t test. *$p < 0.05$, **$p < 0.01$, ***$p < 0.001$.

(E) IF of cortical/forebrain-, midbrain-, and hindbrain/spinal-cord-associated markers in neuronal cultures differentiated from sorted GFP-expressing NPC populations (scale bar, 100 μm). L, GFP^{LOW}; M, GFP^{MID}; H, GFP^{HIGH}.

See also Figure S4.

remained stable in the GFP^{HIGH} NPCs, and *AXIN2* expression did not increase in the GFP^{LOW} NPCs over ten passages (Figure S3D). During the course of ten passages, the forebrain markers *FOXG1*, *SIX3*, and *OTX2* were expressed in the GFP^{LOW} NPCs, but not in the GFP^{HIGH} NPCs (Figure S3E). Conversely, the hindbrain-associated genes *IRX3*, *EN1*, and *HOXB4* were stably expressed in the GFP^{HIGH} NPCs, but were not elevated in the GFP^{LOW} NPCs during the period of ten passages (Figure S3E). In sum, these data indicate that the positional identity of NPCs is stable during long-term culture.

The Level of Endogenous WNT Activity Instructs the Neuronal Differentiation Potential

We wanted to determine whether the level of endogenous WNT signaling present in NPCs conferred a regional bias as they were expanded and subsequently differentiated to neurons in vitro. To address this issue, FC-purified GFP^{HIGH}, GFP^{MID}, and GFP^{LOW} hTOP-19 NPCs were expanded for four passages and then differentiated to neurons (Figure 3A). After 4 weeks of differentiation, all three cell populations generated cells with a neuronal morphology (Figure S4A). Additionally, IF demonstrated

that each NPC population yielded similar numbers of MAP2$^+$ and B3T$^+$ neurons (Figures S4B and S4C). Importantly, gene expression (Figures 3B–3D) and IF analysis (Figure 3E) of neurons generated from these different WNT reporter NPC populations revealed distinct regional identities. Neurons generated from GFP^{LOW} NPCs expressed the highest levels of *FOXG1* (a marker of neurons with telencephalic identity), *SATB2* (labels cortical neurons of layers II/III), *CTIP2* (expressed by striatal medium spiny neurons), *EMX1* (a marker for pyramidal neurons of the cerebral cortex), *CUX1* (expressed in layer IV-II late-born/upper-layer cortical neurons), and TBR1 (labels cortical neurons, especially those associated with layer VI). By comparison, GFP^{MID} NPCs differentiated into neurons with a midbrain phenotype, including expression of the midbrain GABAergic-associated marker GATA3 and the midbrain dopaminergic (mDA)-related markers *LMX1A/1B* (regulate mDA progenitor proliferation, specification, and differentiation), *NURR1* (specifies neurotransmitter identity of mDA neurons), *PITX3* (regulates *tyrosine hydroxylase* [*TH*] expression in mDA neurons), and *TH* (the enzyme responsible for generation of L-DOPA, which is a precursor for the neurotransmitter dopamine). Finally, neurons differentiated from GFP^{HIGH} NPCs expressed the highest levels of hindbrain/spinal-cord-associated genes, such as HOXA2, HOXB4, and *HOXB6*, as well as the motor neuron marker MNX1 (also known as HB9).

Exogenous Modulation of WNT Signaling Influences NPC Positional Identity and Reduces Heterogeneity in Neuronal Differentiation

The above analysis demonstrates that endogenous WNT signaling activity correlates with A/P regional identity of NPCs. To determine the extent to which WNT signaling is instructive in conferring regional bias, we used several methods to perturb WNT signaling during NPC generation. Specifically, we differentiated four independent hPSC lines (H9, HUES9, HES3, and RiPSC; Warren et al., 2010) to NPCs while activating or inhibiting WNT signaling with CHIR 98104 (CHIR, a potent inhibitor of GSK-3β) and IWP2, respectively (Figure 4A). Activation of WNT signaling with CHIR treatment led to an increase in embryoid body (EB) size, whereas inhibition of endogenous WNT signaling through IWP2 treatment resulted in a decrease in EB size (Figures S5A and S5B), consistent with the known role of canonical WNT signaling in promoting proliferation in hESC-derived neurospheres (Davidson et al., 2007). CHIR-treated and IWP2-treated NPCs expressed levels of the pan-neural markers SOX1, SOX2, and NESTIN similar to those observed for untreated NPCs (Figures S5C–S5E).

Although there was no effect of WNT signal perturbations on the formation of SOX1$^+$, SOX2$^+$, and NESTIN$^+$ NPCs, CHIR or IWP2 treatment influenced the A/P expression profile of NPCs. Expression of the anterior marker *FOXG1* decreased in a dose-dependent manner with CHIR treatment, but increased with IWP2 treatment (Figure 4B). Conversely, the levels of the posterior marker *HOXB4* increased in a concentration-dependent manner with CHIR treatment, but decreased with IWP2 treatment (Figure 4C). The expression of A/P markers was also influenced by CHIR and IWP2 treatment across all hPSC lines tested (Figures 4D–4G). Specifically, expression of the anterior markers FOXG1, FORSE-1, *SIX3*, *DLX2*, OTX2, and PAX6 was higher in IWP2-treated cells, whereas expression of the posterior markers *IRX3*, HOXA2, and HOXB4 was higher in CHIR-treated cells. To eliminate the possibility that the posteriorizing effect of CHIR was not due to the activation of other signaling pathways that act through GSK3 (Jope and Johnson, 2004), we also generated NPCs in the presence of WNT3a (Willert, 2008). Similar to the effect of CHIR on A/P gene expression of NPCs, addition of WNT3a during NPC formation led to an increase in expression of the posterior genes *LMX1A*, *EN1*, *IRX3*, and *HOXB4*, and a decrease in expression of the anterior genes *FOXG1*, *SIX3*, *DLX2*, and *OTX2* (Figure S5F). These data demonstrate that exogenous activation or inhibition of canonical WNT signaling can be used to control the positional patterning of NPCs in differentiating hPSCs. Additionally, the observation that inhibition of endogenous WNT signaling with IWP2 during NPC generation reduced the expression of genes associated with posterior identity suggests that endogenous WNT signaling specifies a posterior identity, consistent with its known function in CNS development.

To examine whether patterning of NPCs imposed by exogenous WNT manipulation was stable, we cultured CHIR- and IWP2-treated NPCs in the absence of these exogenous signals for ten passages (>50 days) (Figures S6A and S6B). After ten passages, the expression level of the forebrain marker *FOXG1* remained unchanged in NPCs that were generated in the presence of IWP2 (Figure S6C). Along similar lines, the expression level of the hindbrain marker *HOXB4* remained constant over ten passages of the NPCs that were generated in the presence of CHIR (Figure S6D). Therefore, continued WNT pathway modulation during prolonged culture was not required to maintain the regional identity of NPCs. Furthermore, we examined the ability of NPCs to alter their positional identity after NPC formation. To test this, we treated regionally specified NPCs with CHIR or IWP2 for ten passages after NPC formation (Figures S6A and S6B). Addition of CHIR to anterior-specified NPCs (i.e., NPCs formed in the presence of IWP2) had no effect on *FOXG1* or *HOXB4* expression (Figures S6C and S6D). Likewise, IWP2 treatment of posterior-patterned NPCs (i.e., NPCs formed in the presence of

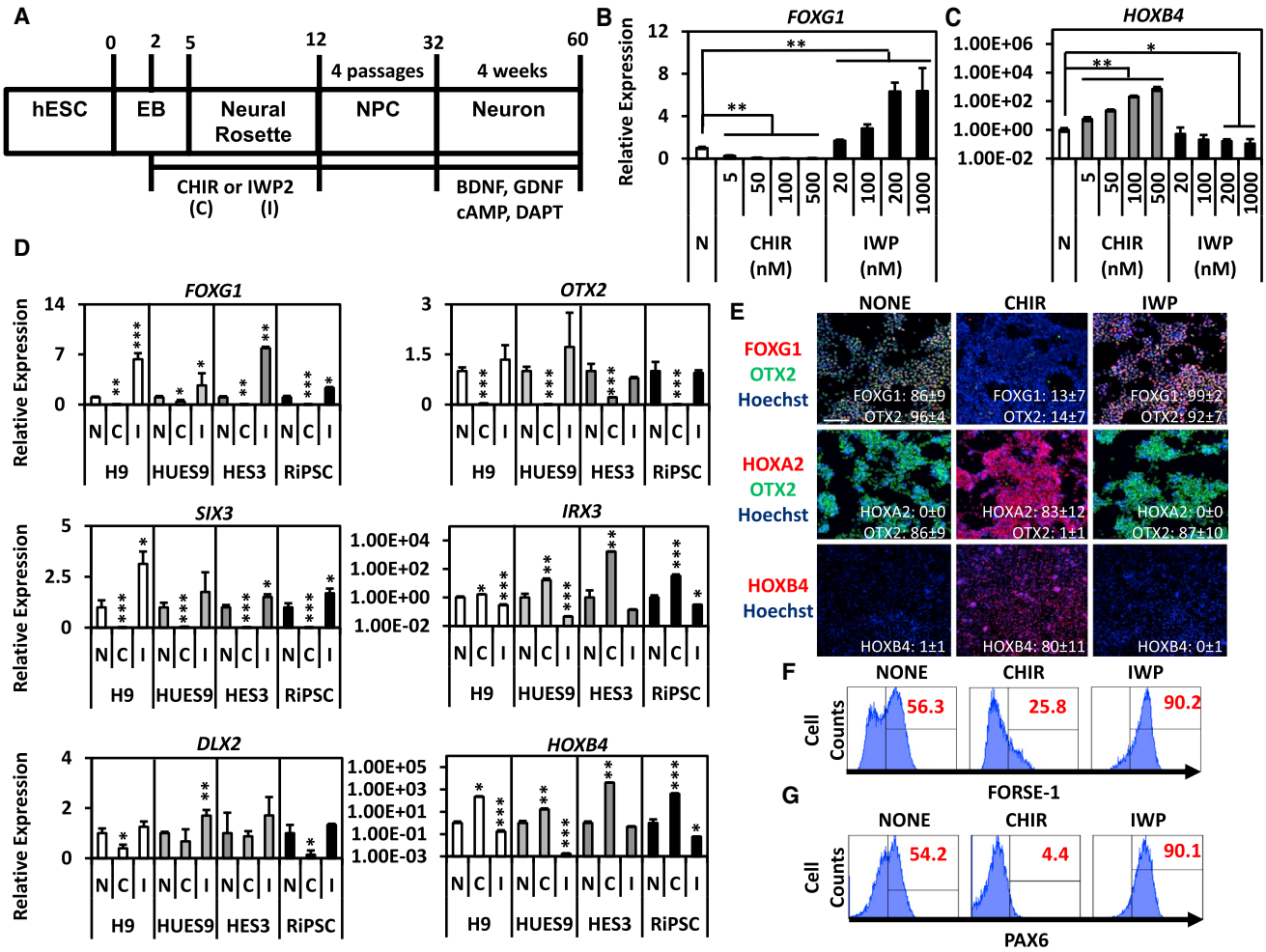

Figure 4. Exogenous Manipulation of WNT Signaling Reduces Heterogeneity in NPC Cultures

(A) Outline of the experimental protocol. CHIR or IWP2 was added during day 2 of neural differentiation. CHIR- and IWP2-treated and untreated NPCs were expanded for four passages prior to differentiation to neurons.

(B and C) Gene-expression analysis of (B) *FOXG1* and (C) *HOXB4* in NPC cultures derived from H9 hPSCs in the presence of varying levels of CHIR and IWP2.

(D) A/P gene expression in 500 nM CHIR- and 1,000 nM IWP2-treated and untreated NPC cultures derived from H9, HUES9, HES3, and RiPSC hPSCs (mean ± SEM, n = 3 independent experiments). Populations were compared with untreated (N) cells using Student's t test. *p < 0.05, **p < 0.01, ***p < 0.001.

(E) IF of A/P-related markers in 500 nM CHIR- and 1,000 nM IWP2-treated and untreated NPC cultures (scale bar, 100 μm).

(F and G) FC of (F) FORSE-1 and (G) PAX6 in 500 nM CHIR- and 1,000 nM IWP2-treated and untreated NPC cultures. Isotype controls used are listed in Table S5. N, none; C, CHIR 98014; I, IWP2.

See also Figure S5.

CHIR) did not change their regional identity (Figures S6C and S6D). Collectively, these data suggest that the effect of exogenous WNT signaling on NPC patterning is imparted early during their generation and NPCs are unable to interconvert between positional identities during subsequent expansion.

We subsequently investigated whether NPCs generated with IWP2 or CHIR treatment retained their regional phenotype upon differentiation to neurons. IWP2- and CHIR-treated NPCs were expanded for four passages and then subjected to the neuronal differentiation protocol. IF (Figure 5A) and gene expression (Figure S5G) revealed that IWP2- and CHIR-treated NPCs generated similar numbers of $B3T^{+}$ neurons compared with untreated NPCs. However, neurons generated from IWP2-treated NPCs expressed higher levels of the forebrain- and

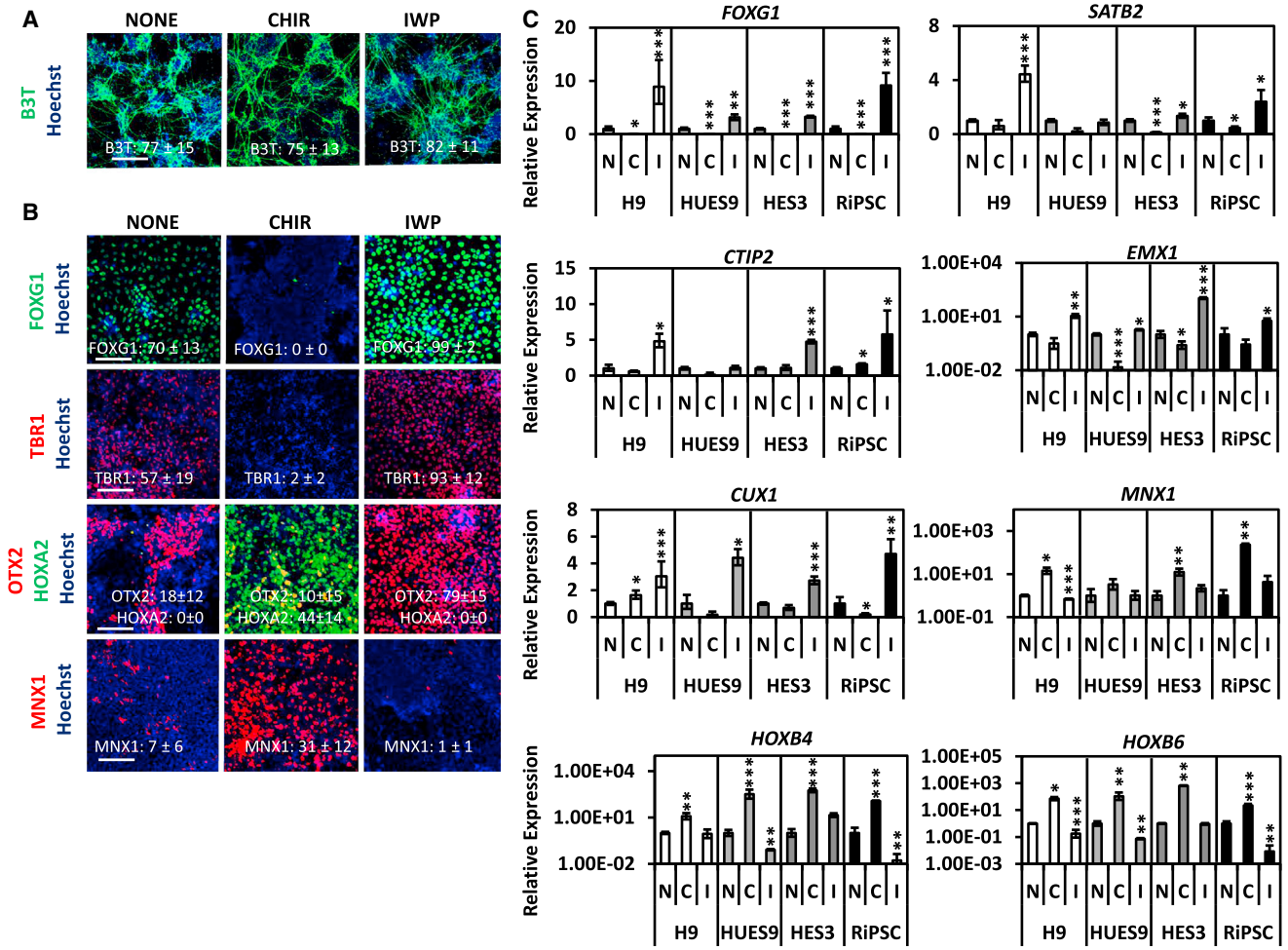

Figure 5. Analysis of Neurons Derived from CHIR- and IWP2-Treated and Untreated NPC Cultures

(A) IF of mature neuronal markers B3T in neuronal cultures differentiated from 500 nM CHIR- and 1,000 nM IWP2-treated and untreated NPC cultures derived from H9 hPSCs (scale bar, 100 μm).

(B) IF of cortical-, forebrain-, midbrain-, hindbrain-, and spinal-cord-related neuronal genes in neurons differentiated from 500 nM CHIR- and 1,000 nM IWP2-treated and untreated NPC cultures derived from H9 hPSCs (scale bar, 100 μm).

(C) Expression of cortical-, forebrain-, midbrain-, hindbrain-, and spinal-cord-related neuronal genes in neurons differentiated from 500 nM CHIR- and 1,000 nM IWP2-treated and untreated NPC cultures derived from H9, HUES9, HES3, and RiPSC hPSCs (mean ± SEM, n = 4 independent experiments). Populations were compared with neurons differentiated from untreated (N) NPCs using Student's t test. *p < 0.05, **p < 0.01, ***p < 0.001.

cortical-related neuronal markers FOXG1, TBR1, *SATB2*, *CTIP2*, *EMX1*, *CUX1*, and *OTX2* compared with neurons generated from CHIR-treated or -untreated NPCs (Figures 5B and 5C). On the other hand, neurons generated from CHIR-treated NPCs expressed higher levels of the hindbrain- and spinal-cord-specific markers HOXA2, *HOXB4*, *HOXB6*, and MNX1 (Figures 5B and 5C). Together, our results indicate that NPCs retain their regional identity over multiple passages and manifest that identity in differentiated neuron cultures.

Although we were able to generate NPC and neuron cultures with distinct anterior and posterior identities, we did not observe cell populations expressing markers associated with a midbrain phenotype. We speculated that this notable absence of midbrain cell types may have been the consequence of endogenous WNT signaling activities that influence the extent to which exogenous WNT signaling imparts A/P identities. To eliminate the contribution of any endogenous WNT signaling during NPC generation and fine-tune the level of WNT signaling activity, we treated differentiating cultures (hPSCs to NPCs) with IWP2 simultaneously with increasing concentrations of CHIR. Analysis of the gene-expression profile of NPCs derived at various concentrations of CHIR revealed that we could

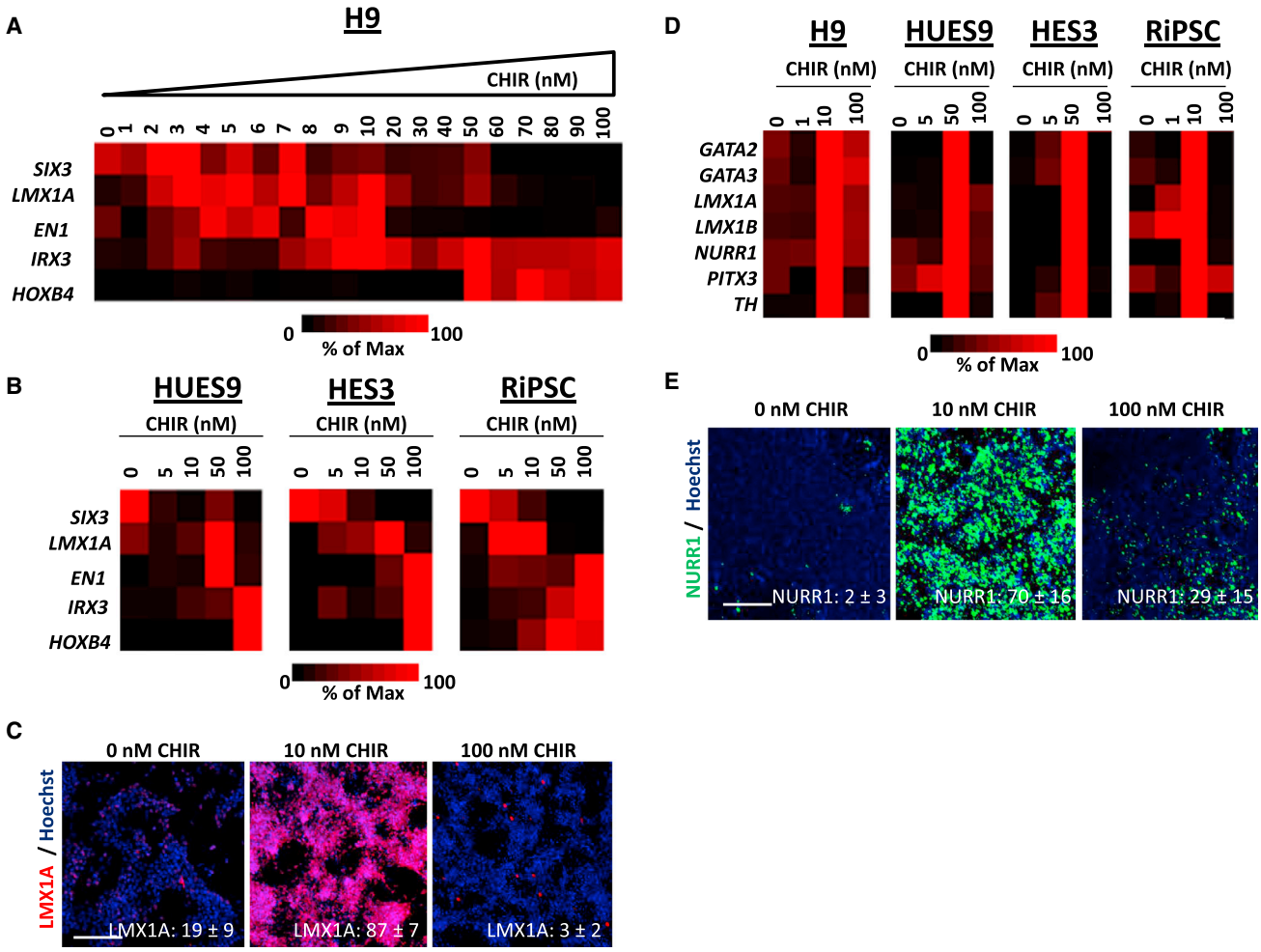

Figure 6. Specification of the Midbrain Neural Phenotype through Precise Exogenous Manipulation of WNT Signaling

(A and B) Gene-expression analysis of A/P-related genes in NPCs generated from (A) H9 (mean, n = 3 technical replicates) and (B) HUES9, HES3, and RiPSC (mean, n = 3 independent experiments) hPSCs in the presence of 1,000 nM IWP2 and various concentrations of CHIR. The data are displayed in a heatmap where black corresponds to minimum expression levels and red corresponds to maximum levels. For each gene analyzed, the expression levels were normalized to the sample with the highest expression level.

(C) IF of LMX1A expression in NPCs generated from H9 hPSCs in the in the presence of 1,000 nM IWP2 and various concentrations of CHIR (scale bar, 100 μm).

(D) Gene-expression analysis of midbrain-related genes in neuronal cultures differentiated from NPCs treated with various CHIR concentrations (mean; H9, n = 3 independent experiments; HUES9, HES3, RiPSC, n = 4 independent experiments).

(E) IF of NURR1 expression in NPCs generated from H9 hPSCs in the in the presence of 1,000 nM IWP2 and various concentrations of CHIR (scale bar, 100 μm).

See also Figure S6.

specify the A/P positional identity of NPCs by precisely controlling the level of exogenous WNT signaling (Figures 6A–6C). In all hPSC lines tested, induction of NPCs with a midbrain phenotype occurred at a narrow CHIR concentration range, with the precise CHIR range varying slightly between hPSC lines. CHIR concentrations significantly lower or higher than these optima led to the production of NPCs with an anterior/forebrain or hindbrain/spinal-cord phenotype, respectively.

We differentiated these NPCs of specific positional fate to neurons. Expression of the midbrain neuronal-related markers *GATA2*, *GATA3*, *LMX1A*, *LMX1B*, NURR1, *PITX3*, and *TH* peaked at a CHIR concentration of 10 nM for NPCs generated from H9 or RiPSC hPSCs, and a CHIR concentration of 50 nM for NPCs generated from HUES9 or HES3 hPSCs (Figures 6D and 6E). Together, these data indicate that by selecting the precise level of extrinsic WNT signaling in the context of suppressed endogenous

WNT signaling, we could generate hPSC-derived NPCs and neurons with midbrain characteristics.

DISCUSSION

hPSCs and their derivative NPCs share the ability to self-renew indefinitely while retaining the potential to differentiate into mature cell types, although the potential of NPCs is restricted to cells of the CNS, including neurons, astrocytes, and oligodendrocytes. Our study demonstrates that NPCs are additionally restricted by their positional identity. As in development of the CNS, where establishment of the A/P axis early during neural tube formation confers a specific positional identity on naive neuroepithelial cells, NPCs acquire similar positional information from their microenvironment. Importantly, despite their apparent homogeneous appearance and lack of a clear 3D architecture, NPCs in cell culture acquire and stably maintain this A/P positional identity. In contrast to this stable identity of NPCs, where individual and heterogeneous states coexist and do not interconvert, ESCs exist in a metastable state in which individual cells exhibit oscillatory expression of transcription factors (Cahan and Daley, 2013; Canham et al., 2010; de Souza, 2012; Galvin-Burgess et al., 2013; Narsinh et al., 2011; Stewart et al., 2006), correlating with a bias to either self-renew or differentiate. Importantly, we show that NPC positional identity and specific neuronal differentiation potential are retained over prolonged expansion (>50 days) in culture.

The WNT signaling pathway is a primary determinant in assigning an A/P positional identity to NPCs. This instructional cue is imparted early during NPC generation and once this identity is established, it is stable and cannot be altered through exogenous manipulation of the WNT pathway. Using a WNT reporter line, we show that endogenous WNT signaling is highly variable among individual cells as they acquire a NPC phenotype, with cells of posterior identity expressing WNT reporter activity. In addition to expressing markers of posteriorly fated NPCs, most notably genes of the HOX gene cluster, these cells also express multiple WNT ligands. In contrast, NPCs with anterior identity, as detected by a lack of WNT reporter activity, express multiple WNT antagonists. These differences in expression of WNT agonist and antagonist resemble those observed in the developing neural tube in vivo, with posterior tissues expressing WNT proteins and anterior tissues expressing WNT antagonists such as DKK1 and FRZB (Hashimoto et al., 2000; Leyns et al., 1997).

These opposing WNT signals generate an endogenous gradient of WNT activity, which divides the embryonic neural tube along the A/P axis into distinct progenitor domains, each of which gives rise to specific regionalized neurons (Ciani and Salinas, 2005; Kiecker and Niehrs, 2001; Nordström et al., 2002). These progenitor domains have regionally specific gene-expression profiles and differentiation predispositions despite similar levels of expression of the pan-neural markers SOX1 and SOX2 (Pevny et al., 1998; Wood and Episkopou, 1999; Zappone et al., 2000). Here, we showed that NPCs exhibited a broad range of endogenous WNT activity that conferred specific regionalized fates despite comparable expression levels of SOX1 and SOX2, perhaps mimicking the same developmental events that are seen during early in vivo neural tube development. Therefore, the local WNT microenvironment tightly regulates the WNT activity status and hence the positional identity of NPCs.

A somewhat unexpected implication of these gene-expression patterns is that WNT signaling appears to be acting cell autonomously, with WNT signaling activity restricted to those cells expressing *WNT* genes. Although WNT signaling activity is present in a graded fashion in these NPC cultures, WNT proteins are acting in an autocrine rather than paracrine manner. Furthermore, expression of WNT antagonists may mute the response in cells near or adjacent to WNT secreting cells. A more careful analysis of this cell-based system will likely yield important mechanistic insights into the dynamic nature of WNT signaling during development.

This restricted WNT signaling activity observed in NPC cultures is consistent with the notion that WNT proteins act locally (Habib et al., 2013) and exhibit minimal, if any, extracellular diffusion. A recent study demonstrated that flies expressing an engineered membrane-tethered Wingless (a fly WNT protein) are viable and normally patterned, suggesting that the spread of Wingless is dispensable for patterning and growth (Alexandre et al., 2014). Similarly, in our cell-based system, WNT proteins act locally and do not signal to distant cells. In addition, expression of WNT antagonists in the WNT^{-} populations may act to block paracrine WNT signaling activity. This local WNT activity is not the result of the physical separation of distinct WNT expressing domains, since this localized activity is retained in a mixed and seemingly homogeneous cell culture system.

While endogenous WNT signaling activity is a major source of heterogeneity among individual NPCs, exogenous manipulation of this signaling pathway can be exploited to impart specific positional identities to NPCs during their generation from hPSCs, thereby reducing cellular heterogeneity. Activation of WNT signaling with purified WNT3a protein or a GSK-3β inhibitor (CHIR98014) led to the generation of NPCs with a hindbrain/spinal cord identity, whereas inhibition of WNT signaling with a PORCN inhibitor (IWP2) to block endogenous WNT protein processing led to the generation of NPCs

with a forebrain phenotype. As shown in this and other studies (Li et al., 2009; Pankratz et al., 2007), in the absence of any WNT pathway manipulations, NPCs generated form hPSCs are generally biased toward an anterior fate, suggesting that endogenous WNT signaling in these culture systems is relatively low and insufficient to promote posterior fates. Consequently, ectopic activation of WNT signaling produces a prominent shift from an anterior to a posterior fate. In contrast, in the absence of WNT signaling (through IWP2 addition), the relative increase of anterior-related markers, though statistically significant, is less pronounced.

Although exogenous manipulation of WNT signaling can be used to reduce NPC heterogeneity, the window during which this manipulation is effective is limited. Specifically, we find that WNT signaling imparts positional identity early during NPC generation, likely during the rosette stage, in which the cell population most closely resembles the early developing neural tube. Once an NPC culture is established and propagated over multiple passages, A/P positional identity is stable and recalcitrant to exogenous manipulations of WNT signaling. Therefore, the identity, concentration, and timing of factors (e.g., WNTs) added during NPC generation are critical to produce homogeneous cultures.

Although WNT signaling plays a prominent role in A/P patterning of the neural tube, few studies have extensively examined the influence of WNT on the A/P positional identity of hPSC-derived NPCs and neurons. To date, most studies have relied on FGF8 (Yan et al., 2005; Yang et al., 2008) or retinoic acid (RA) (Dimos et al., 2008; Hu and Zhang, 2009; Li et al., 2005, 2008; Singh Roy et al., 2005) to generate posterior neural populations, such as midbrain dopaminergic and spinal cord motor neurons, respectively, from hPSCs. Similar to the approach we used in our study, two groups recently used a specific concentration of the GSK3β inhibitor CHIR99021 (an analog to the GSK3β inhibitor used in this study) to generate midbrain dopaminergic neurons from hPSCs (Kirkeby et al., 2012; Kriks et al., 2011). However, the ability of this compound to generate stable NPC populations from different areas of A/P axis was not extensively studied. We demonstrated that through precise chemical modulation of WNT signaling, we could control the A/P positional identity of hPSC-derived NPCs. Moreover, we demonstrated that these NPCs retained their positional specificity as they were differentiated to neurons in vitro. It should also be noted that previous studies (Hu and Zhang, 2009; Yan et al., 2005) have relied on the activation of SHH signaling in order to generate ventral neurons, such as mDA and motor neurons. In this study, we demonstrated that we were able to generate these ventral neuronal subtypes without exogenous modulation of SHH signaling. This suggests the possibility that endogenous SHH signaling may regulate the dorsal-ventral (D/V) identity of hPSC-derived NPCs and neurons analogously to the manner in which endogenous WNT signaling regulates their A/P identity. Nonetheless, our study serves as proof-of-principle that modulation of developmental signaling pathways, such as WNT and SHH, can be exploited to refine the A/P and D/V identity of NPCs and neurons.

Our findings regarding the positional restriction of NPCs have important implications for the study and application of these cells. Several studies have described the transplantation of hPSC-derived NPCs into animal models of Parkinson's disease, Huntington's disease, amyotrophic lateral sclerosis, and spinal cord injury (Kim et al., 2013; Lindvall and Kokaia, 2010). However, few of these studies have described a successful long-term reduction in the symptoms associated with these disorders (Kim et al., 2013; Lindvall and Kokaia, 2010). Interestingly, several of these studies relied on NPCs generated by dual SMAD inhibition, which results in NPCs of an anterior telencephalic identity (Chambers et al., 2009), which may explain the lack of symptomatic improvement in animal models of disorders associated with the midbrain, hindbrain, and spinal cord. We speculate that future animal transplantation studies that utilize regionally specific and stably expandable NPCs, such as those generated in this study, will result in a significant improvement in the cognitive and motor deficits associated with these neurological disorders.

In summary, we determined that endogenous WNT signaling influences the heterogeneity, regional characteristics, and differential potential of hPSC-derived NPCs. In addition, we showed that precise exogenous modulation of WNT signaling during neural differentiation of hPSCs results in a homogeneous NPC population with a specific positional identity. Importantly, manipulation of endogenous and exogenous WNT signaling will allow for the development of defined methods for generating transplantable hPSC-derived NPCs for specific regions of the entire A/P axis of the neural tube. Furthermore, this study suggests that modulation of other developmental signaling pathways, including BMP, FGF, and SHH, can be exploited to further refine the positional identity of NPCs and neurons. In the future, these regionally specific NPCs will greatly enhance the translational potential of hPSCs for neural-related therapies.

EXPERIMENTAL PROCEDURES

Cells and Culture Conditions

Media compositions and sources for all cell lines are listed in the Supplemental Experimental Procedures. All work with hPSCs was reviewed and approved by the Stem Cell Research Oversight Committee of the University of California, San Diego (project numbers 100210ZX and 090807ZX).

Generation of WNT Reporter hESCs

The infection and generation of WNT reporter hESCs are described in the Supplemental Experimental Procedures. The lentiviral construct that was used to generate the WNT reporter line contained a 7xTCF-eGFP construct and puromycin resistance gene (Fuerer and Nusse, 2010). High titer lentivirus was produced as previously described (Miyoshi et al., 1998; Zufferey et al., 1998). Clones were screened for robust TOP-GFP expression upon WNT3a stimulation and a normal euploid karyotype.

NPC Generation, Expansion, and Differentiation

The methods used for the generation, expansion, and neuronal differentiation of hPSC-derived NPCs are described in the Supplemental Experimental Procedures and Brafman (2014).

qPCR

Details regarding the methods used for qPCR are provided in the Supplemental Experimental Procedures. RNA was isolated using TRIzol and reverse transcription was performed with the use of the qScript cDNA Supermix. qPCR was carried out using Taqman Probes (Table S4) and the TaqMan Fast Universal PCR Master Mix on a 7900HT Real-Time PCR machine. Gene expression was normalized to 18 s rRNA levels. All experiments were preformed with three technical replicates.

IF and FC

Detailed protocols for IF and FC are provided in the Supplemental Experimental Procedures. The antibodies used are listed in Table S5. Quantification of images was performed by counting a minimum of nine fields at 20× magnification. Image quantification of the data is presented as the average of these fields ± SD.

High-Throughput RNA-Seq

RNA-seq of RNA from TOP-GFP$^+$ and TOP-GFP$^-$ NPCs was performed as described in the Supplemental Experimental Procedures, and differential gene-expression analysis was performed with TopHat and Cufflinks (Trapnell et al., 2012, 2013). Reads per kilobase per million mapped (RPKM) values were calculated for each gene and used as an estimate of expression levels. The raw RNA-seq data are provided in Table S1.

SUPPLEMENTAL INFORMATION

Supplemental Information includes Supplemental Experimental Procedures, six figures, and five tables and can be found with this article online at http://dx.doi.org/10.1016/j.stemcr.2014.10.004.

AUTHOR CONTRIBUTIONS

N.M., J.C., and D.A.B. designed and conceived the study. N.M., J.C., K.W., and D.A.B. performed experiments. N.M., J.C., K.W., T.G., and D.A.B. analyzed data. N.M., J.C., K.W., and D.A.B. wrote the manuscript.

ACKNOWLEDGMENTS

D.A.B. was supported by funding from the UCSD Stem Cell Program and a gift from Michael and Nancy Kaehr. This research was supported in part by the California Institute for Regenerative Medicine (RT2-01889 and RB1-01406) and was made possible in part by a CIRM Major Facilities grant (FA1-00607) to the Sanford Consortium for Regenerative Medicine.

Received: February 8, 2014
Revised: October 13, 2014
Accepted: October 14, 2014
Published: November 13, 2014

REFERENCES

Alexandre, C., Baena-Lopez, A., and Vincent, J.P. (2014). Patterning and growth control by membrane-tethered Wingless. Nature *505*, 180–185.

Blauwkamp, T.A., Nigam, S., Ardehali, R., Weissman, I.L., and Nusse, R. (2012). Endogenous Wnt signalling in human embryonic stem cells generates an equilibrium of distinct lineage-specified progenitors. Nat. Commun. *3*, 1070.

Brafman, D.A. (2014). Generation, expansion, and differentiation of human pluripotent stem cell (hPSC) derived neural progenitor cells (NPCs). Methods Mol. Biol. Published online July 26, 2014. http://dx.doi.org/10.1007/7651_2014_90.

Cahan, P., and Daley, G.Q. (2013). Origins and implications of pluripotent stem cell variability and heterogeneity. Nat. Rev. Mol. Cell Biol. *14*, 357–368.

Canham, M.A., Sharov, A.A., Ko, M.S., and Brickman, J.M. (2010). Functional heterogeneity of embryonic stem cells revealed through translational amplification of an early endodermal transcript. PLoS Biol. *8*, e1000379.

Chambers, S.M., Fasano, C.A., Papapetrou, E.P., Tomishima, M., Sadelain, M., and Studer, L. (2009). Highly efficient neural conversion of human ES and iPS cells by dual inhibition of SMAD signaling. Nat. Biotechnol. *27*, 275–280.

Chen, B., Dodge, M.E., Tang, W., Lu, J., Ma, Z., Fan, C.W., Wei, S., Hao, W., Kilgore, J., Williams, N.S., et al. (2009). Small molecule-mediated disruption of Wnt-dependent signaling in tissue regeneration and cancer. Nat. Chem. Biol. *5*, 100–107.

Ciani, L., and Salinas, P.C. (2005). WNTs in the vertebrate nervous system: from patterning to neuronal connectivity. Nat. Rev. Neurosci. *6*, 351–362.

Davidson, K.C., Jamshidi, P., Daly, R., Hearn, M.T., Pera, M.F., and Dottori, M. (2007). Wnt3a regulates survival, expansion, and maintenance of neural progenitors derived from human embryonic stem cells. Mol. Cell. Neurosci. *36*, 408–415.

de Souza, N. (2012). Taming stem cell heterogeneity. Nat. Methods *9*, 645.

Dimos, J.T., Rodolfa, K.T., Niakan, K.K., Weisenthal, L.M., Mitsumoto, H., Chung, W., Croft, G.F., Saphier, G., Leibel, R., Goland, R., et al. (2008). Induced pluripotent stem cells generated from patients with ALS can be differentiated into motor neurons. Science *321*, 1218–1221.

Dottori, M., and Pera, M.F. (2008). Neural differentiation of human embryonic stem cells. Methods Mol. Biol. *438*, 19–30.

Drukker, M., Tang, C., Ardehali, R., Rinkevich, Y., Seita, J., Lee, A.S., Mosley, A.R., Weissman, I.L., and Soen, Y. (2012). Isolation of primitive endoderm, mesoderm, vascular endothelial and trophoblast progenitors from human pluripotent stem cells. Nat. Biotechnol. *30*, 531–542.

Dykstra, B., Kent, D., Bowie, M., McCaffrey, L., Hamilton, M., Lyons, K., Lee, S.J., Brinkman, R., and Eaves, C. (2007). Long-term propagation of distinct hematopoietic differentiation programs in vivo. Cell Stem Cell *1*, 218–229.

Elkabetz, Y., Panagiotakos, G., Al Shamy, G., Socci, N.D., Tabar, V., and Studer, L. (2008). Human ES cell-derived neural rosettes reveal a functionally distinct early neural stem cell stage. Genes Dev. *22*, 152–165.

Fuerer, C., and Nusse, R. (2010). Lentiviral vectors to probe and manipulate the Wnt signaling pathway. PLoS ONE *5*, e9370.

Galvin-Burgess, K.E., Travis, E.D., Pierson, K.E., and Vivian, J.L. (2013). TGF-β-superfamily signaling regulates embryonic stem cell heterogeneity: self-renewal as a dynamic and regulated equilibrium. Stem Cells *31*, 48–58.

Gaspard, N., and Vanderhaeghen, P. (2010). Mechanisms of neural specification from embryonic stem cells. Curr. Opin. Neurobiol. *20*, 37–43.

Germain, N., Banda, E., and Grabel, L. (2010). Embryonic stem cell neurogenesis and neural specification. J. Cell. Biochem. *111*, 535–542.

Habib, S.J., Chen, B.C., Tsai, F.C., Anastassiadis, K., Meyer, T., Betzig, E., and Nusse, R. (2013). A localized Wnt signal orients asymmetric stem cell division in vitro. Science *339*, 1445–1448.

Hashimoto, H., Itoh, M., Yamanaka, Y., Yamashita, S., Shimizu, T., Solnica-Krezel, L., Hibi, M., and Hirano, T. (2000). Zebrafish Dkk1 functions in forebrain specification and axial mesendoderm formation. Dev. Biol. *217*, 138–152.

Hong, S.H., Rampalli, S., Lee, J.B., McNicol, J., Collins, T., Draper, J.S., and Bhatia, M. (2011). Cell fate potential of human pluripotent stem cells is encoded by histone modifications. Cell Stem Cell *9*, 24–36.

Hu, B.Y., and Zhang, S.C. (2009). Differentiation of spinal motor neurons from pluripotent human stem cells. Nat. Protoc. *4*, 1295–1304.

Huang, S., Guo, Y.P., May, G., and Enver, T. (2007). Bifurcation dynamics in lineage-commitment in bipotent progenitor cells. Dev. Biol. *305*, 695–713.

Jiang, Y., Zhang, M.J., and Hu, B.Y. (2012). Specification of functional neurons and glia from human pluripotent stem cells. Protein Cell *3*, 818–825.

Jiang, W., Zhang, D., Bursac, N., and Zhang, Y. (2013). WNT3 is a biomarker capable of predicting the definitive endoderm differentiation potential of hESCs. Stem Cell Rep. *1*, 46–52.

Jope, R.S., and Johnson, G.V. (2004). The glamour and gloom of glycogen synthase kinase-3. Trends Biochem. Sci. *29*, 95–102.

Kiecker, C., and Niehrs, C. (2001). A morphogen gradient of Wnt/beta-catenin signalling regulates anteroposterior neural patterning in Xenopus. Development *128*, 4189–4201.

Kim, S.U., Lee, H.J., and Kim, Y.B. (2013). Neural stem cell-based treatment for neurodegenerative diseases. Neuropathology *33*, 491–504.

Kirkeby, A., Grealish, S., Wolf, D.A., Nelander, J., Wood, J., Lundblad, M., Lindvall, O., and Parmar, M. (2012). Generation of regionally specified neural progenitors and functional neurons from human embryonic stem cells under defined conditions. Cell Rep. *1*, 703–714.

Koch, P., Kokaia, Z., Lindvall, O., and Brüstle, O. (2009). Emerging concepts in neural stem cell research: autologous repair and cell-based disease modelling. Lancet Neurol. *8*, 819–829.

Kriks, S., Shim, J.W., Piao, J., Ganat, Y.M., Wakeman, D.R., Xie, Z., Carrillo-Reid, L., Auyeung, G., Antonacci, C., Buch, A., et al. (2011). Dopamine neurons derived from human ES cells efficiently engraft in animal models of Parkinson's disease. Nature *480*, 547–551.

Leyns, L., Bouwmeester, T., Kim, S.H., Piccolo, S., and De Robertis, E.M. (1997). Frzb-1 is a secreted antagonist of Wnt signaling expressed in the Spemann organizer. Cell *88*, 747–756.

Li, X.J., Du, Z.W., Zarnowska, E.D., Pankratz, M., Hansen, L.O., Pearce, R.A., and Zhang, S.C. (2005). Specification of motoneurons from human embryonic stem cells. Nat. Biotechnol. *23*, 215–221.

Li, X.J., Hu, B.Y., Jones, S.A., Zhang, Y.S., Lavaute, T., Du, Z.W., and Zhang, S.C. (2008). Directed differentiation of ventral spinal progenitors and motor neurons from human embryonic stem cells by small molecules. Stem Cells *26*, 886–893.

Li, X.J., Zhang, X., Johnson, M.A., Wang, Z.B., Lavaute, T., and Zhang, S.C. (2009). Coordination of sonic hedgehog and Wnt signaling determines ventral and dorsal telencephalic neuron types from human embryonic stem cells. Development *136*, 4055–4063.

Lindvall, O., and Kokaia, Z. (2010). Stem cells in human neurodegenerative disorders—time for clinical translation? J. Clin. Invest. *120*, 29–40.

Liu, H., and Zhang, S.C. (2011). Specification of neuronal and glial subtypes from human pluripotent stem cells. Cell. Mol. Life Sci. *68*, 3995–4008.

Miyoshi, H., Blömer, U., Takahashi, M., Gage, F.H., and Verma, I.M. (1998). Development of a self-inactivating lentivirus vector. J. Virol. *72*, 8150–8157.

Narsinh, K.H., Sun, N., Sanchez-Freire, V., Lee, A.S., Almeida, P., Hu, S., Jan, T., Wilson, K.D., Leong, D., Rosenberg, J., et al. (2011). Single cell transcriptional profiling reveals heterogeneity of human induced pluripotent stem cells. J. Clin. Invest. *121*, 1217–1221.

Nat, R., and Dechant, G. (2011). Milestones of directed differentiation of mouse and human embryonic stem cells into telencephalic neurons based on neural development in vivo. Stem Cells Dev. *20*, 947–958.

Nordström, U., Jessell, T.M., and Edlund, T. (2002). Progressive induction of caudal neural character by graded Wnt signaling. Nat. Neurosci. *5*, 525–532.

Pankratz, M.T., Li, X.J., Lavaute, T.M., Lyons, E.A., Chen, X., and Zhang, S.C. (2007). Directed neural differentiation of human

embryonic stem cells via an obligated primitive anterior stage. Stem Cells *25*, 1511–1520.

Peljto, M., and Wichterle, H. (2011). Programming embryonic stem cells to neuronal subtypes. Curr. Opin. Neurobiol. *21*, 43–51.

Pevny, L.H., Sockanathan, S., Placzek, M., and Lovell-Badge, R. (1998). A role for SOX1 in neural determination. Development *125*, 1967–1978.

Sangiorgi, E., and Capecchi, M.R. (2008). Bmi1 is expressed in vivo in intestinal stem cells. Nat. Genet. *40*, 915–920.

Singh Roy, N., Nakano, T., Xuing, L., Kang, J., Nedergaard, M., and Goldman, S.A. (2005). Enhancer-specified GFP-based FACS purification of human spinal motor neurons from embryonic stem cells. Exp. Neurol. *196*, 224–234.

Stewart, M.H., Bossé, M., Chadwick, K., Menendez, P., Bendall, S.C., and Bhatia, M. (2006). Clonal isolation of hESCs reveals heterogeneity within the pluripotent stem cell compartment. Nat. Methods *3*, 807–815.

Trapnell, C., Roberts, A., Goff, L., Pertea, G., Kim, D., Kelley, D.R., Pimentel, H., Salzberg, S.L., Rinn, J.L., and Pachter, L. (2012). Differential gene and transcript expression analysis of RNA-seq experiments with TopHat and Cufflinks. Nat. Protoc. *7*, 562–578.

Trapnell, C., Hendrickson, D.G., Sauvageau, M., Goff, L., Rinn, J.L., and Pachter, L. (2013). Differential analysis of gene regulation at transcript resolution with RNA-seq. Nat. Biotechnol. *31*, 46–53.

Uwanogho, D., Rex, M., Cartwright, E.J., Pearl, G., Healy, C., Scotting, P.J., and Sharpe, P.T. (1995). Embryonic expression of the chicken Sox2, Sox3 and Sox11 genes suggests an interactive role in neuronal development. Mech. Dev. *49*, 23–36.

Warren, L., Manos, P.D., Ahfeldt, T., Loh, Y.H., Li, H., Lau, F., Ebina, W., Mandal, P.K., Smith, Z.D., Meissner, A., et al. (2010). Highly efficient reprogramming to pluripotency and directed differentiation of human cells with synthetic modified mRNA. Cell Stem Cell *7*, 618–630.

Willert, K.H. (2008). Isolation and application of bioactive Wnt proteins. Methods Mol. Biol. *468*, 17–29.

Wood, H.B., and Episkopou, V. (1999). Comparative expression of the mouse Sox1, Sox2 and Sox3 genes from pre-gastrulation to early somite stages. Mech. Dev. *86*, 197–201.

Wu, J., and Tzanakakis, E.S. (2012). Contribution of stochastic partitioning at human embryonic stem cell division to NANOG heterogeneity. PLoS ONE *7*, e50715.

Yan, Y., Yang, D., Zarnowska, E.D., Du, Z., Werbel, B., Valliere, C., Pearce, R.A., Thomson, J.A., and Zhang, S.C. (2005). Directed differentiation of dopaminergic neuronal subtypes from human embryonic stem cells. Stem Cells *23*, 781–790.

Yang, D., Zhang, Z.J., Oldenburg, M., Ayala, M., and Zhang, S.C. (2008). Human embryonic stem cell-derived dopaminergic neurons reverse functional deficit in parkinsonian rats. Stem Cells *26*, 55–63.

Zappone, M.V., Galli, R., Catena, R., Meani, N., De Biasi, S., Mattei, E., Tiveron, C., Vescovi, A.L., Lovell-Badge, R., Ottolenghi, S., and Nicolis, S.K. (2000). Sox2 regulatory sequences direct expression of a (beta)-geo transgene to telencephalic neural stem cells and precursors of the mouse embryo, revealing regionalization of gene expression in CNS stem cells. Development *127*, 2367–2382.

Zhang, S.C. (2006). Neural subtype specification from embryonic stem cells. Brain Pathol. *16*, 132–142.

Zhang, S.C., Li, X.J., Johnson, M.A., and Pankratz, M.T. (2008). Human embryonic stem cells for brain repair? Philos. Trans. R. Soc. Lond. B Biol. Sci. *363*, 87–99.

Zufferey, R., Dull, T., Mandel, R.J., Bukovsky, A., Quiroz, D., Naldini, L., and Trono, D. (1998). Self-inactivating lentivirus vector for safe and efficient in vivo gene delivery. J. Virol. *72*, 9873–9880.

Stem Cell Reports, Volume *3*

Supplemental Information

Endogenous WNT Signaling Regulates hPSC-Derived Neural Progenitor Cell Heterogeneity and Specifies Their Regional Identity

Noel Moya, Josh Cutts, Terry Gaasterland, Karl Willert, and David A. Brafman

SUPPLEMENTAL EXPERIMENTAL PROCEDURES

Cells and culture conditions. All media components were from Life Technologies unless otherwise noted. For hPSC culture, the following media were used: mouse embryonic fibroblast (MEF) (1X high glucose DMEM, 10% fetal bovine serum, 1% (v/v) L-glutamine penicillin/streptomycin). H9/HES3/RiPSC hPSCs (1X DMEM-F12, 20% (v/v) Knockout Serum Replacement, 1% (v/v) non-essential amino acids, 0.5% (v/v) glutamine, 120 μM 2-mercaptoethanol [Sigma]). HUES9 (1 x Knockout DMEM, 10% (v/v) Knockout Serum Replacement, 10% (v/v) human plasmanate (Chapin Healthcare, Anaheim CA, USA) 1% (v/v) non-essential amino acids, 0.5% (v/v) glutamine, 55 μM 2-mercaptoethanol [Sigma]); All hPSC lines were maintained on feeder layers of mitotically inactivated MEFs ($2x10^4/cm^2$; Millipore). All hPSC cultures were supplemented with 30 ng/ml FGF2 (Life Technologies). MEF-CM was produced by culturing hPSC medium on MEFs for 24 hr followed by sterile filtering. Cells were routinely passaged with Accutase (Millipore), washed, and replated at a density $4.25 \times 10^4/cm^2$.

Generation of Wnt reporter hESCs. The lentiviral construct that was used to generate the WNT reporter line contained a 7xTCF-eGFP construct and puromycin resistance gene[25]. High titer lentivirus was produced as previously described[97, 98]. HUES9 hESCs were infected overnight with lentivirus. Infected pools were selected with puromycin (0.5 μg/ml) for 2 weeks. For generation of clonal hESC lines, transduced pools were then treated with 200 ng/ml purified mouse WNT3a[99] for 48 hours. Cells were dissociated with Accutase for 5 min at 37°C, triturated, and passed through a 40 μm cell strainer. Cells were then washed twice with FACS buffer (PBS, 10 mM EDTA, and 2% FBS) and resuspended at a maximum concentration of 5×10^6 cells per 100 ul. Single TOP-GFP+ cells were sorted into a Matrigel (BD)-coated 96 well plated with MEF-CM supplemented with 5 μM ROCK inhibitor Y27632 (Stemgent) and 30 ng/ml FGF2. After expansion, a total of 45 clones were screened for: (1) robust TOP-GFP expression upon WNT3a stimulation and (2) normal euploid karyotype.

Neural progenitor cell (NPC) generation, expansion, and differentiation. To initiate neural differentiation, hPSCs were cultured on Matrigel (BD Biosciences) in MEF-CM supplemented with 30 ng/ml FGF2 or TeSR™2 (Stem Cell Technologies). Cells were then detached with treatment with Accutase (Millipore) for 5 min and resuspended in neural induction media (1% N2/1% B27 without vitamin A/DMEM:F12) supplemented with 5 μM Y-267632 (Stemgent), 50 ng/ml recombinant mouse Noggin (R&D Systems), 0.5 μM Dorsomorphin (Tocris Bioscience)]. Next, 7.5×10^5 cells were pipetted to each well of a 6-well ultra low attachment plates (Corning). The plates were then placed on an orbital shaker set at 95 rpm in a 37°C/5% CO2 tissue culture incubator. The next day, the cells formed spherical clusters (embryoid bodies [EBs]) and the media was changed to neural induction media with 50 ng/ml recombinant mouse Noggin and 0.5 μM Dorsomorphin. The media was subsequently changed every other day. After 5 days in suspension culture, the EBs were then transferred to a 10 cm dish coated (3 x 6 wells per 10 cm dish) with growth factor reduced Matrigel (1:25 in KnockOut DMEM; BD Biosciences) for attachment. The plated EBs were cultured in neural induction media with 50 ng/ml recombinant mouse Noggin and 0.5 μM Dorsomorphin for an additional 7 days. Neural rosettes were cut out by dissection under an EVOS (Life Technologies) microscope. Dissected rosettes were incubated in Accutase for 5 min and then triturated to single cells with a 1 mL pipet. Rosettes were then plated onto poly-L-ornithine (PLO; 10 μg/mL; Sigma) and mouse laminin (Ln; 5 μg/mL; Sigma) coated dishes at a density of 12,500 cells/cm^2 in neural induction media supplemented with 10 ng/mL mouse FGF2 and 10 ng/ml mouse EGF2 (R&D Systems). IWP2 (Stemgent) and CHIR 98014 (CHIR; Axon Medchem) were added 2 days after EB formation. For routine maintenance, NPCs were passaged onto PLO/Ln coated plates at a density of 10,000 cells/cm^2 in neural induction media supplemented with 10 ng/mL mouse FGF2 and 10 ng/ml mouse EGF2. TOP-GFP sorted as well as IWP2- and CHIR-treated NPCs were derived and

maintained in the absence of FGF2 and EGF2. For neuronal differentiation, NPCs were dissociated with Accutase for 5 min at 37°C, triturated, and plated onto PLO/Ln coated plates at a density of 100,000 cells/cm^2. Cells were cultured in neuronal differentiation media (0.5% N2/0.5% B27 without vitamin A/DMEM:F12) supplemented with 20 ng/ml BDNF (R&D Systems), 20 ng/ml GDNF (R&D Systems), 1 µM DAPT (Tocris Bioscience), and 0.5 mM , dibutyrl-cAMP (db-cAMP; Sigma) for 4 weeks.

Quantitative PCR (Q-PCR). RNA was isolated from cells using TRIzol (Life Technologies), and treated with DNase I (Life Technologies) to remove traces of genomic DNA. Reverse transcription was performed with qScript cDNA Supermix (Quanta Biosciences). Quantitative PCR was carried out using TaqMan probes (Life Technologies) and TaqMan Fast Universal PCR Master Mix (Life Technologies) on a 7900HT Real Time PCR machine (Life Technologies), with a 10 min gradient to 95°C followed by 40 cycles at 95°C for 15s and 60°C for 1 min. Taqman gene expression assay primers (Life Technologies; **Table S4**) were used. Gene expression was normalized to 18S rRNA levels. Delta Ct values were calculated as $C_t^{target} - C_t^{18s}$. All experiments were performed with three technical replicates. Relative fold changes in gene expression were calculated using the $2^{-\Delta\Delta Ct}$ method[100]. Data are presented as the average of the biological replicates ± standard error of the mean (S.E.M).

Immunofluorescence. Cultures were gently washed twice with staining buffer (PBS w/ 1% (w/v) BSA) prior to fixation. Cultures were then fixed for 15 min at room temperature (RT) with fresh paraformaldeyde (4% (w/v)). The cultures were washed twice with staining buffer and permeabilized with 0.2% (v/v) Triton-X-100 in stain buffer for 20 min at 4°C. Cultures were then washed twice with staining buffer. Primary antibodies were incubated overnight at 4°C and then washed twice with stain buffer at RT. Secondary antibodies were incubated at RT for 1 hr. Antibodies used are listed in **Table S5**. Nucleic acids were stained for DNA with Hoechst 33342 (2 µg/ml; Life Technologies) for 5 min at room temperature. Imaging was performed using an automated confocal microscope (Olympus Fluoview 1000 with motorized stage). Quantification of images was performed by counting a minimum of 9 fields at 20x magnification. Image quantification of the data is presented as the average of these fields ± standard deviation (S.D.).

Flow cytometry and cell replating. Cells were dissociated with Accutase for 5 min at 37°C, triturated, and passed through a 40 µm cell strainer. Cells were then washed twice with FACS buffer (PBS, 10 mM EDTA, and 2% FBS) and resuspended at a maximum concentration of 5 x 10^6 cells per 100 ul. One test volume of antibody was added for each 100 µl cell suspension (**Table S5**). Cells were stained for 30 min on ice, washed, and resuspended in stain buffer. Cells were analyzed and sorted with a FACSCanto or FACSAria (BD Biosciences). Flow cytometry data was analyzed with FACSDiva software (BD Biosciences). Isotype negative controls are listed in **Table S4**. For sorting experiments in which cells were separated on the basis of GFP expression, wild-type (WT) non-fluorescing cells were used as a negative control. For replating experiments, cells were stained with appropriate antibodies and sorted into FACS buffer with 5µM Y27632 (Stemgent). Sorted cells were replated at the appropriate density and media with 10 µM Y27632.

High throughput RNA sequencing (RNA-seq). Total RNA from FACS sorted TOP-GFP$^+$ and TOP-GFP$^-$ NPCs were isolated, depleted of genomic DNA and rRNA and fragmented to ~200 bp by RNase III. After ligating the Adaptor Mix, fragmented RNA was converted to the first strand cDNA by ArrayScript Reverse Transcriptase (Ambion), size selected (100-200bp) by gel electrophoresis, and amplified by PCR using adaptor-specific primers. Deep sequencing was performed on an Illumina Genome Analyzer II. Analysis of genome-wide expression data was performed as previously described[101, 102]. Briefly, raw reads from two biologically independent samples were aligned to the reference human genome (hg19) using

TopHat. Cufflinks was used to assemble individual transcripts from the mapped reads. Cuffmerge was used to merge the assembled transcripts from the two biologically independent samples. Cuffdiff was used to calculate gene expression levels and test for the statistical significance of differences in gene expression. Reads per kilobase per million mapped reads (RPKM) were calculated for each gene and used as an estimate of expression levels.

LEGENDS FOR SUPPLEMENTAL FIGURES

Supplemental Figure S1, related to Figure 1. Generation of clonal WNT reporter hESC lines. (a) Schematic of TOP-GFP lentiviral construct. (b) Flow cytometry analysis of expanded clones after 48 hour treatment with 15 nM purified mouse WNT3a. Clone 19 (hTOP-19) displayed the highest expression of GFP after WNT3a treatment. (c) Karyotype analysis of hTOP-19. Chromosome spread indicated a normal euploid female karyotype (46XX). (d) Flow cytometry analysis of hTOP-19 hESCs treated with various concentrations of WNT3a. (e) Flow cytometry analysis of hTOP-19 hESCs treated with GSK3β inhibitor BIO. (f) Flow cytometry analysis of GFP expression in reporter expressing NPCs after 48 hours of treatment with 15 nM WNT3a or 1000 nM IWP2. Abbreviations: NFC=Non-fluorescing channel.

Supplemental Figure S2, related to Figure 1. Differentiation of hPSCs to neural progenitor cells (NPCs) and neurons. (a) Overview of differentiation protocol for differentiation of hPSCs to NPCs and neurons. The soluble factors, substrate, and culture media at each stage are shown. (b) Immunofluorescence of OCT4, NANOG, SOX2, and SOX1 in hESCs and NPCs (scale bar = 100 µm). (c) Flow cytometry analysis of SOX1 and SOX2 expression in hESCs and NPCs. Isotype controls used are listed in **Table S2** (d) Phase contrast images of hESCs and NPCs (scale bar = 100 µm). (e) Gene expression analysis of anterior/posterior (A/P) neural tube related genes in hESCs and NPCs (mean ± S.E.M, n=3 independent experiments). Populations were compared using Student's t-test. * $p<0.05$, ** $p<0.01$, *** $p<0.001$. Flow cytometry analysis of (f) FORSE-1 and (g) PAX6 and (m) in NPCs. Isotype controls used are listed in **Table S5**. (h) Immunofluorescence of HOXB4 in NPCs (scale bar = 200 µm). (i) Immunofluorescence of B3T in neuronal cultures (scale bar = 1 mm). (j) Immunofluorescence of MAP2 and GFAP in neuronal cultures (scale bar = 200 µm). (k) B3T and γ-Aminobutyric acid (GABA) in neurons differentiated from hESCs (scale bar = 200 µm). Abbreviations: NFC=Non-fluorescing channel.

Supplemental Figure S3, related to Figure 2. **Analysis of TOP-GFP expressing NPC populations.** (a) Gene expression analysis of *SOX2* and *NESTIN* (mean ± S.E.M, n=3 independent experiments). (b) Immunofluorescence of NESTIN, SOX1, and SOX2. (c) Reporter expressing NPCs were separated by fluorescence-based cell sorting into GFP^{HIGH} and GFP^{LOW} populations on the basis of GFP expression. GFP^{HIGH} and GFP^{LOW} NPC populations were subsequently cultured for 10 passages (>50 days) and examine for expression of WNT and A/P related genes. (d) Gene expression of WNT target gene *AXIN2* in GFP sorted NPC populations after 5 and 10 passages (mean ± S.E.M, n=3 independent experiments). (e) Gene expression analysis of A/P related genes in GFP sorted NPC populations after 5 and 10 passages (mean ± S.E.M, n=3 independent experiments). Populations were compared using Student's t-test. * $p<0.05$, ** $p<0.01$, *** $p<0.001$. Abbreviations: N.S. = Not statistically significant; L = GFP^{LOW}; M = GFP^{MID}, H = GFP^{HIGH}.

Supplemental Figure S4, related to Figure 3. Analysis of neurons generated from TOP-GFP expressing NPC populations. (a) Phase contrast images of neurons derived from sorted GFP expressing NPC populations (scale bar = 500 µm). (b) Immunofluorescence of mature neuronal markers MAP2 and B3T in neuronal cultures differentiated from sorted GFP^{LOW}, GFP^{MID}, and GFP^{HIGH} NPC populations (scale bar = 200 µm). (c) Gene expression analysis of MAP2 and B3T in neuronal cultures differentiated from sorted GFP^{LOW}, GFP^{MID}, and GFP^{HIGH} NPC populations (mean ± S.E.M, n=4 independent experiments). Populations were compared to using Student's t-test. Abbreviations: N.S. = Not statistically significant

Supplemental Figure S5, related to Figure 4. Analysis of CHIR-, WNT-, IWP2-, and un-treated embryoid bodies, NPCs, and neurons. (a) Phase contrast images and size distribution of embryoid bodies (EBs) generated in 500 nM CHIR-, 1000 nM IWP2-, and un-treated conditions (scale bar = 200 µm). (b) Size

distribution of EBs generated in 500 nM CHIR-, 1000 nM IWP2-, and un-treated conditions. The diameter of 200 EBs was measured for each condition. (c) Gene expression (mean ± S.E.M, n=3 independent experiments), (d) immunofluorescence (scale bar = 100 μm), and (e) flow cytometry analysis of NESTIN, SOX1, and SOX2 of NPCs generated in 500 nM CHIR-, 1000 nM IWP2-, and un-treated conditions. Isotype controls used are listed in **Table S2**. (f) Gene expression analysis of anterior/posterior (A/P) neural tube related genes in NPCs (mean ± S.E.M, n=3 independent experiments) generated in the presence of various WNT concentrations. Populations were compared using Student's t-test. * $p<0.05$, ** $p<0.01$, *** $p<0.001$. (g) Gene expression analysis of MAP2 and B3T in neuronal cultures differentiated from NPCs generated in 500 nM CHIR-, 1000 nM IWP2-, and un-treated conditions (mean ± S.E.M, n=4 independent experiments). Populations were compared to neurons differentiated from untreated (N) NPCs using Student's t-test. Abbreviations: N=None, C=CHIR 98014, I=IWP2, N.S. = Not statistically significant

Supplemental Figure S6, related to Figure 5. Analysis of stability of patterning of NPCs imposed by exogenous WNT manipulation. (a) Posterior-patterned NPCs (i.e. NPCs generated in the presence of 500 nM CHIR) were cultured without CHIR (C-N) or in the presence of 500 nM CHIR (C-C) or 1000 nM IWP2 (C-I) for 10 passages. (b) Anterior-patterned NPCs (i.e. NPCs generated in the presence of 1000 nM IWP2 were cultured without IWP2 (I-N) or in the presence of 500 nM CHIR (I-C) or 1000 nM IWP2 (I-I) for 10 passages. Expression of (c) *FOXG1* and (d) *HOXB4* was assessed in all conditions after 10 passages and compared to initial passage (P0) NPC cultures (mean ± S.E.M, n=3 independent experiments). Populations were compared using Student's t-test. * $p<0.05$, ** $p<0.01$, *** $p<0.001$.

Supplemental Table S1. RNA-seq data of sorted passage 5 GFP^+ and GFP^- NPCs, related to Figure 1. RNA-seq data related to Figure 1c. Genes highlighted in light green were significantly upregulated in TOP GFP- NPCs while genes highlighted in dark green were significantly upregulated in TOP-GFP+ NPCs. Fold changes for each gene are presented as $\log_2$[(TOP-GFP+ RPKM)/(TOP-GFP- RPKM)]. The data in this table is presented in Figure 1c.

Supplemental Table S2. RNA-seq data of WNT pathway components, related to Figure 1. The data in this table is presented in Figure 1D.

Supplemental Table S3. RNA-seq data of A/P related genes, related to Figure 1. The data in this table is presented in Figure 1E.

Supplemental Table S4. TaqMan gene expression assays used in this study.

Supplemental Table S5. Antibodies used in this study.

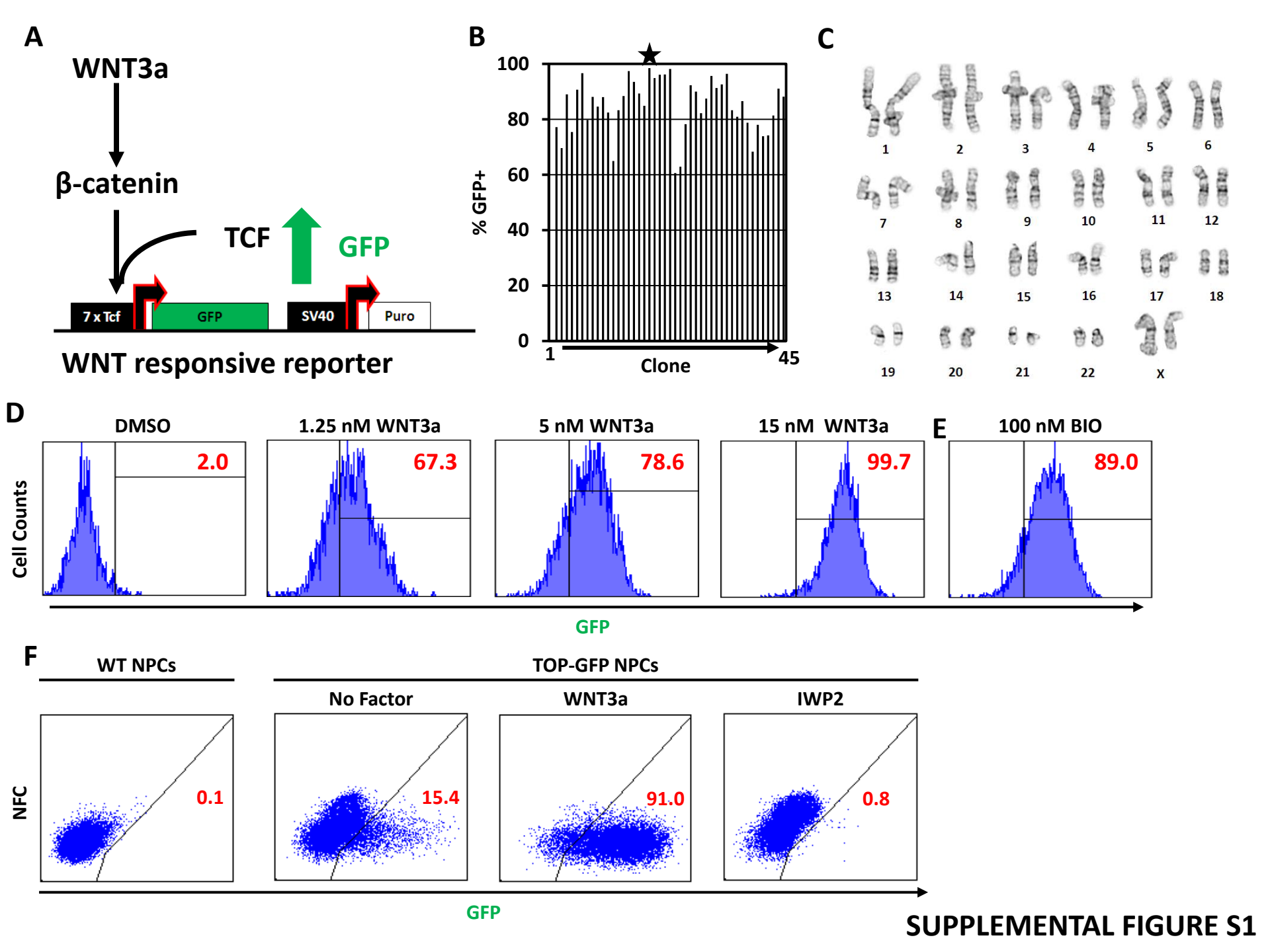

SUPPLEMENTAL FIGURE S1

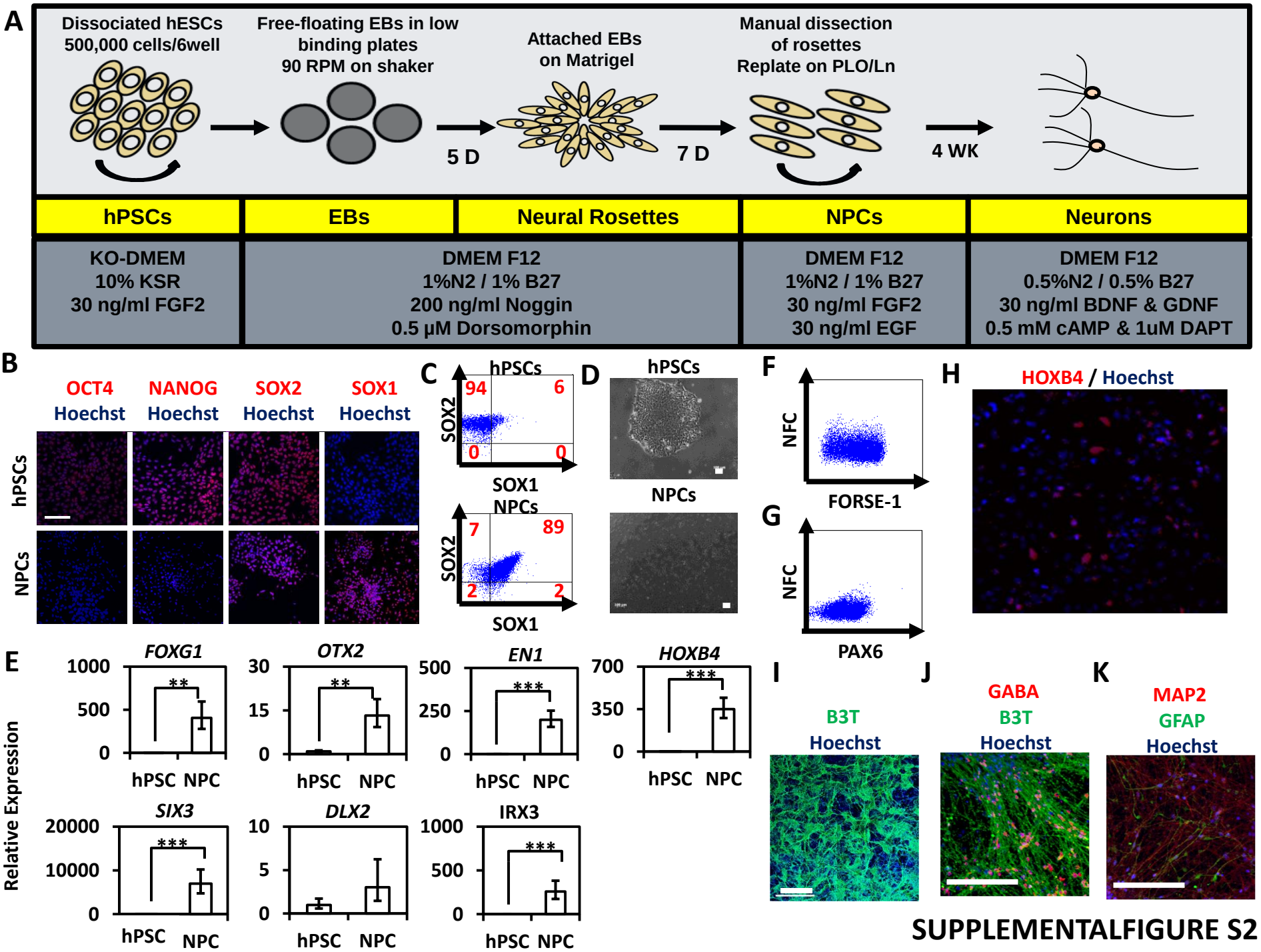

SUPPLEMENTALFIGURE S2

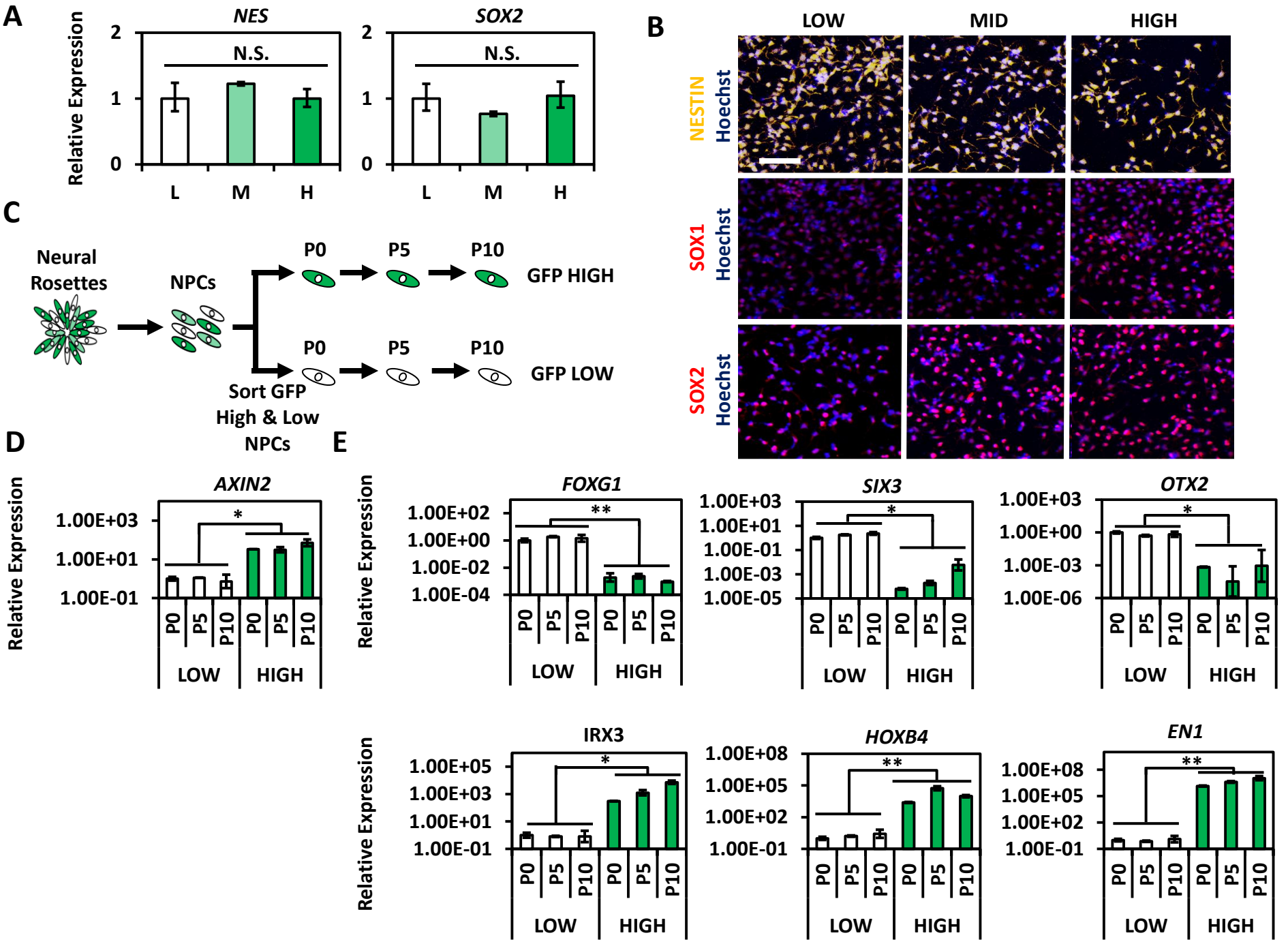

SUPPLEMENTAL FIGURE S3

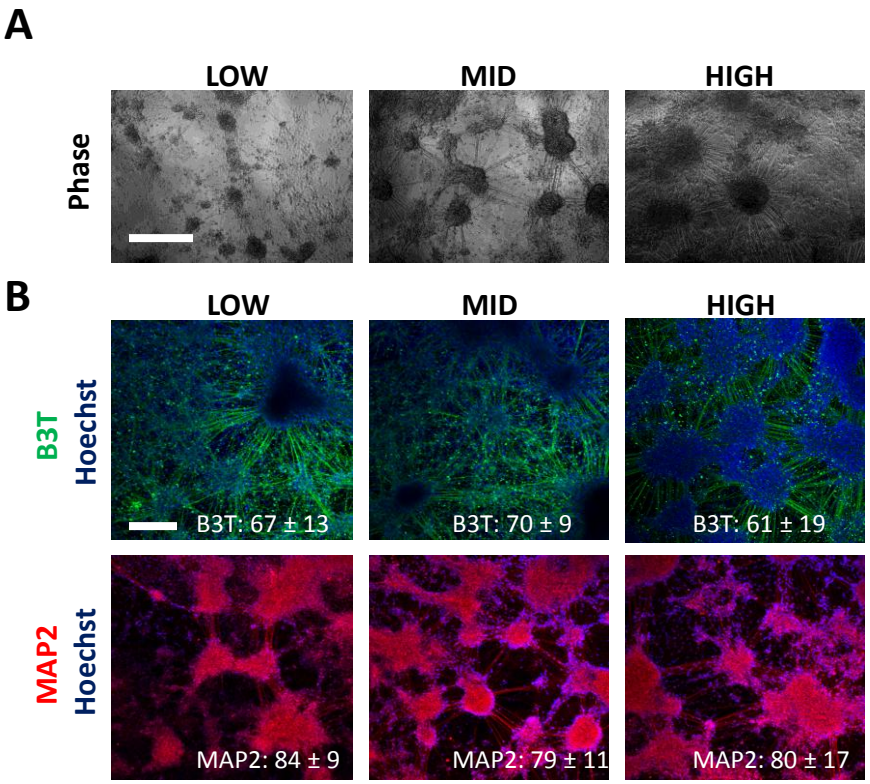

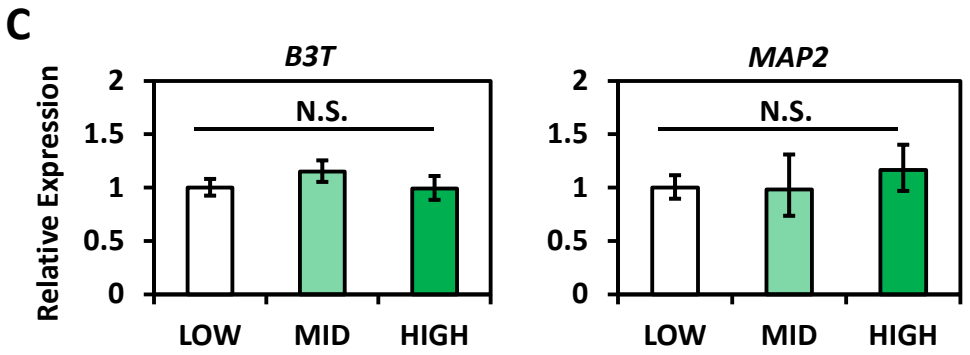

SUPPLEMENTAL FIGURE S4

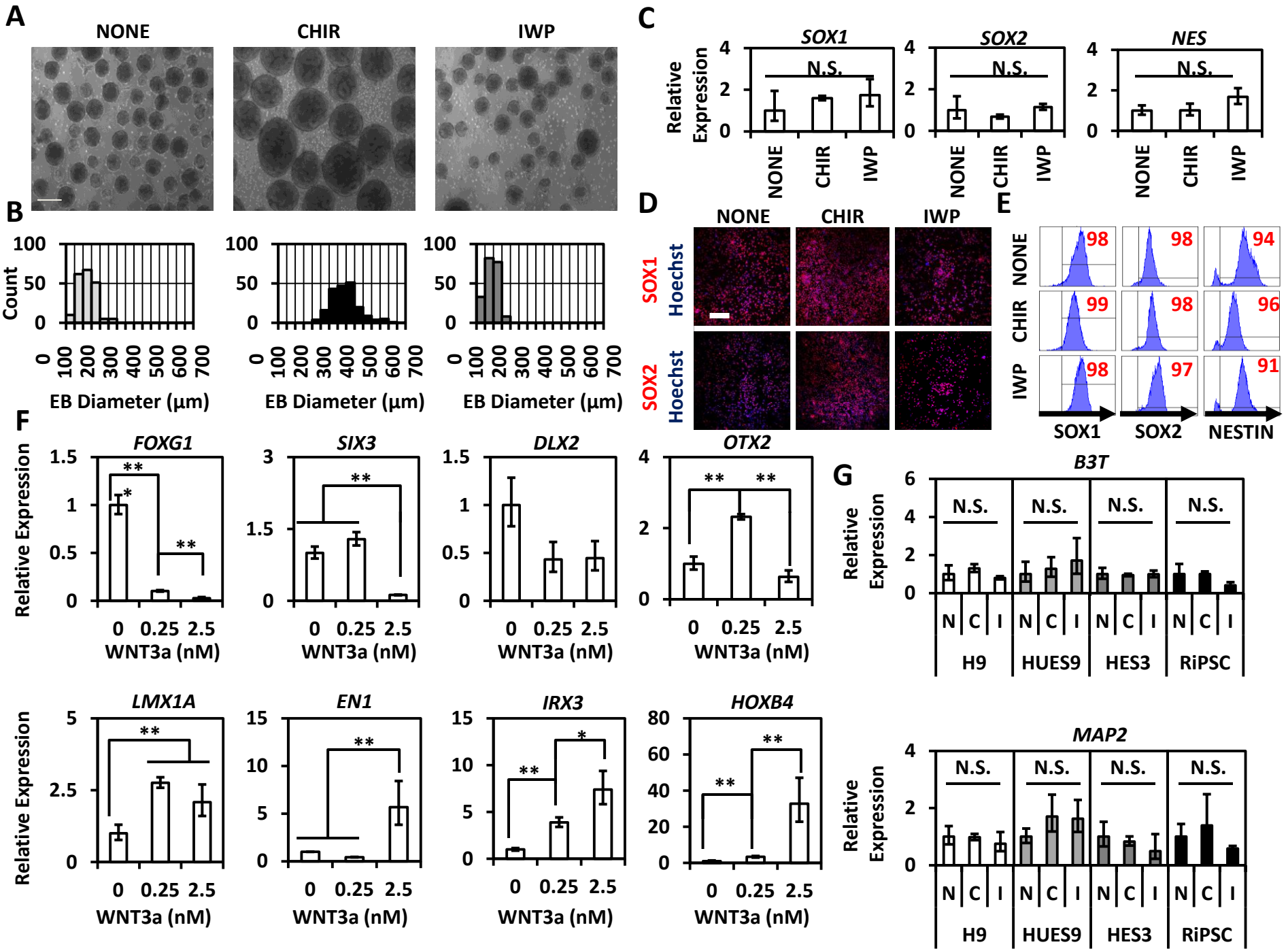

SUPPLEMENTAL FIGURE S5

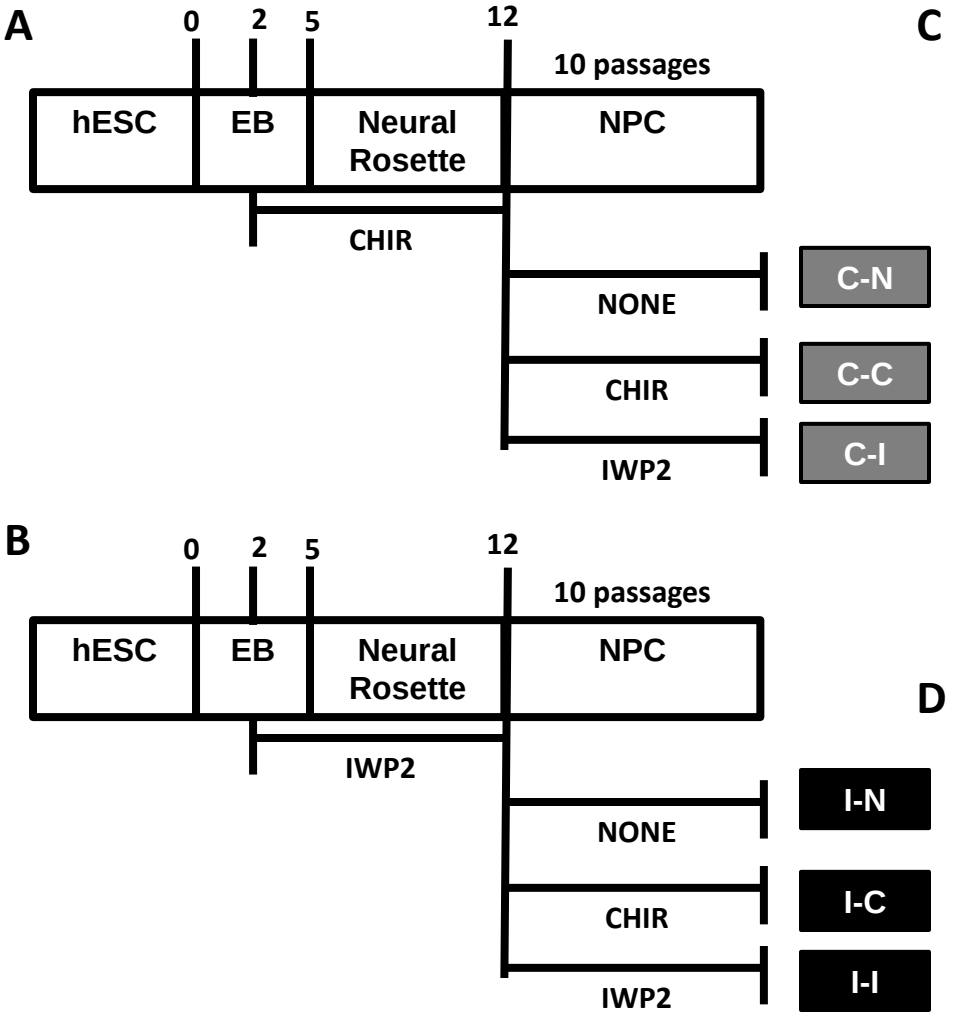

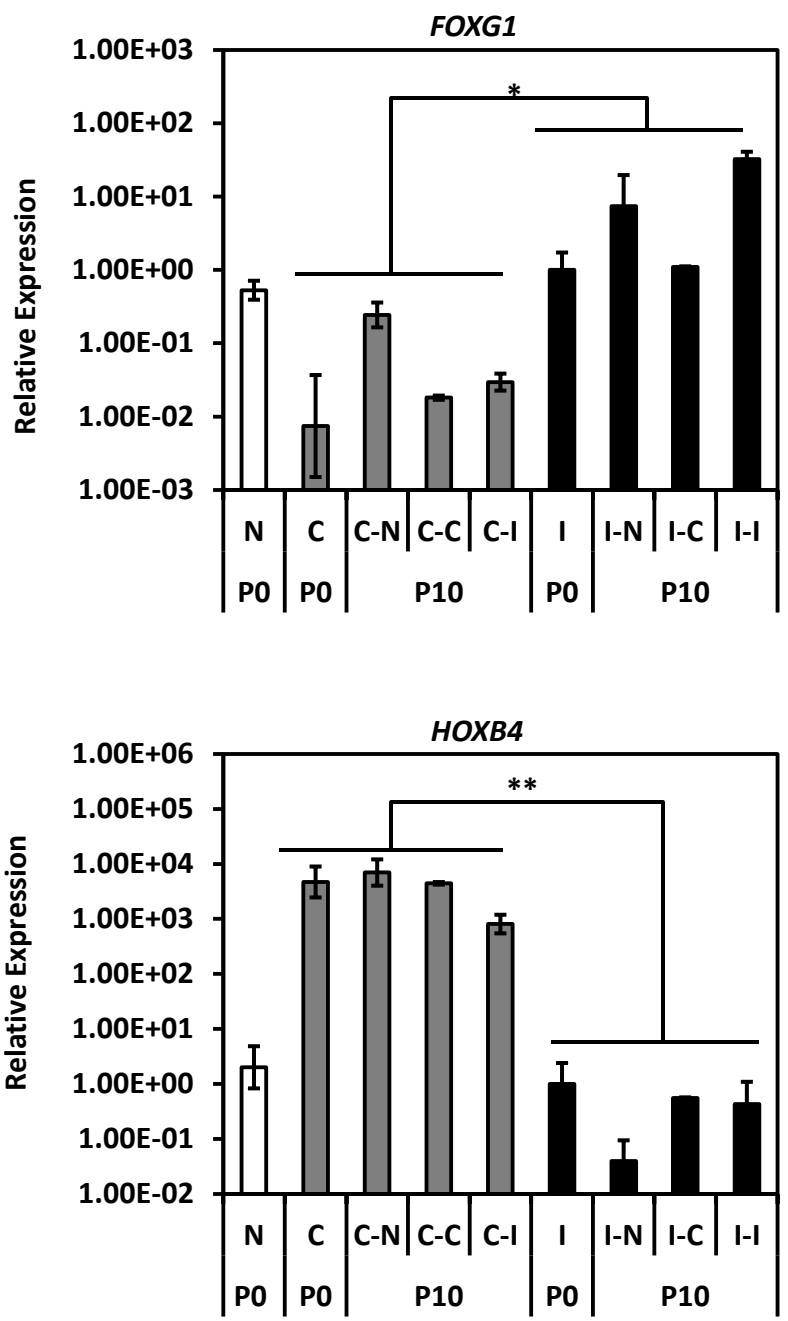

SUPPLEMENTAL FIGURE S6

Gene	ABI Assay
18s	Hs99999901_s1
AXIN2	Hs00610344_m1
CTIP2 (BCL11B)	Hs00256257_m1
CHAT	Hs00252848_m1
CUX1	Hs00738851_m1
DLX2	Hs00269993_m1
EMX1	Hs00417957_m1
EN1	Hs00154977_m1
FGF5	Hs03676587_s1
FOXG1	Hs01850784_s1
GABRA1	Hs00168058_m1
GATA2	Hs00231119_m1
GATA3	Hs00231122_m1
GFAP	Hs00157674_m1
HOXB4	Hs00256884-m1
HOXB6	Hs00980016_m1
IRX3	Hs00735523_m1
LMX1A	Hs00892663_m1
LMX1B	Hs00158750_m1
MAP2	Hs00258900_m1
MNX1 (HB9)	Hs00907365_m1
NES	Hs00707120_s1
NURR1 (NR4A2)	Hs00428691_m1
OTX2	Hs00222238-m1
PITX3	Hs01013935_g1
SATB2	Hs00392652_m1
SIX3	Hs00193667_m1
SOX1	HS01057642_s1
SOX2	Hs01053049_s1
SP5	Hs01370227_mH
TH	Hs00165941_m1
TUBB3	Hs00801390_s1

SUPPLEMENTAL TABLE S4

Antibody	Vendor	Catalog #	Concentration Used
Goat anti-SOX2	Santa Cruz	SC-17320	1:50
Goat anti-OTX2	R&D Systems	AF1979	1:200
Mouse anti-B3T	Fitzgerald	10R-T136A	1:1000
Mouse anti-EN1	DSHB	4G11	1:800
Mouse anti-FORSE-1	DSHB	Concentrate	1:75
Mouse anti-GFAP	Millipore	AB360	1:500
Mouse anti-MNX1	DSHB	81.5C10	1:100
Mouse anti-Nestin	BD	560341	1:10
Mouse anti-SOX1	BD	560749	1:10
Rabbit anti-FOXG1	Abcam	AB18259	1:100
Rabbit anti-GABA	Millipore	AB15415	1:200
Rabbit anti-HOXA2	Sigma	HPA029774	1:200
Rabbit anti-HOXB4	Abcam	AB76093	1:10
Rabbit anti-LMX1A	Abcam	AB139726	1:100
Rabbit anti-MAP2	Millipore	AB5622	1:500
Rabbit anti-NANOG	Santa Cruz	SC-33759	1:50
Rabbit anti-NURR1	Millipore	AB5778	1:200
Rabbit anti-OCT4	Santa Cruz	SC-9081	1:50
Rabbit anti-TBR1	Abcam	AB31940	1:200
Alexa-647 Mouse Anti-SOX2	BD	560294	20 µl per test
PE Mouse anti-Nestin	BD	561230	5 µl per test
PE Mouse anti-PAX6	BD	561552	5 µl per test
PerCp-Cy5.5 Mouse anti-SOX1	BD	561549	5 µl per test
Alexa-647 Mouse IgG2a Isotype Control	BD	558053	20 µl per test
PE Mouse IgG1 Isotype Control	BioLegend	400113	5 ul per test
PE Mouse IgG2a Isotype Control	BD	561552	5 ul per test
PercCp-Cy5.5 MouseIgG1 Isotype Control	BD	550795	5 ul per test
Alexa 647 Donkey Anti-Goat	Life Technologies	A-21447	1:200
Alexa 647 Donkey Anti-Rabbit	Life Technologies	A-31573	1:200
Alexa 647 Donkey Anti-Mouse	Life Technologies	A-31571	1:200
Alexa 546 Donkey Anti-Goat	Life Technologies	A-11056	1:200
Alexa 546 Donkey Anti-Rabbit	Life Technologies	A-10040	1:200
Alexa 546 Donkey Anti-Mouse	Life Technologies	A-10036	1:200
Alexa 488 Donkey Anti-Goat	Life Technologies	A-11055	1:200
Alexa 488 Donkey Anti-Rabbit	Life Technologies	A-21206	1:200
Alexa 488 Donkey Anti-Mouse	Life Technologies	A-21202	1:200

SUPPLEMENTAL TABLE S5